Roles of Growth Hormone and Insulin-like Growth Factor 1 in Mouse Postnatal Growth

Floria Lupu,* Joseph D. Terwilliger,† Kaechoong Lee,‡
Gino V. Segre,‡ and Argiris Efstratiadis*,[1]

**Department of Genetics and Development and *†*Department of Psychiatry and Genome
Center, Columbia University, New York, New York 10032; and *‡*Endocrine Unit,
Massachusetts General Hospital, and Department of Medicine,
Harvard Medical School, Boston, Massachusetts 02114*

To examine the relationship between growth hormone (GH) and insulin-like growth factor 1 (IGF1) in controlling postnatal growth, we performed a comparative analysis of dwarfing phenotypes manifested in mouse mutants lacking GH receptor, IGF1, or both. This genetic study has provided conclusive evidence demonstrating that GH and IGF1 promote postnatal growth by both independent and common functions, as the growth retardation of double *Ghr/Igf1* nullizygotes is more severe than that observed with either class of single mutant. In fact, the body weight of these double-mutant mice is only ~17% of normal and, in absolute magnitude (~5 g), only twice that of the smallest known mammal. Thus, the growth control pathway in which the components of the GH/IGF1 signaling systems participate constitutes the major determinant of body size. To complement this conclusion mainly based on extensive growth curve analyses, we also present details concerning the involvement of the GH/IGF1 axis in linear growth derived by a developmental study of long bone ossification in the mutants.   © 2001 Academic Press

Key Words: growth; growth rate; growth retardation; growth hormone; growth hormone receptor; insulin-like growth factor 1; ossification; chondrocyte.

INTRODUCTION

The growth (increase in size) of a mammalian organism is effected predominantly by proliferative events outbalancing apoptosis and increasing total cell number, with some additional contributions by cell hypertrophy and deposition of extracellular matrix. During mouse development, this process begins in early embryogenesis (blastocyst stage) and lasts until a steady state (balance between proliferation and apoptosis) is reached postnatally, when a mouse attains a determinate body size (~30 g) at about 4–5 months of age.

Growth is brought about by the operation of cellular signaling pathways controlled by growth factors and hormones. Growth factors are produced by many tissues and exert mainly local (autocrine/paracrine) controls that pre-

dominate during embryogenesis, whereas hormones act systemically away from the sites of their production.

Among the classic growth factors, the IGFs (insulin-like growth factors; IGF1 and IGF2) were shown to be members of a major growth-promoting signaling system (reviewed by Efstratiadis, 1998). IGF2 is essential for normal embryonic growth (DeChiara *et al.,* 1990, 1991), whereas IGF1 is a ligand that has a continuous function throughout development (Liu *et al.,* 1993; Baker *et al.,* 1993). Thus, the growth rate of *Igf1* nullizygotes, if they survive, continues to be lower than normal postnatally, as it was during embryogenesis. As a consequence, these mutants, which have ~60% of normal weight at birth (~60%*N*), become ~30%*N* at steady state.

Postnatally, a major growth regulator is growth hormone (GH), which has no apparent embryonic role, despite the presence of its cognate receptor (GHR) in embryos (García-Aragón *et al.,* 1992; Pantaleon *et al.,* 1997). Thus, absence of GH action in mutant animals or experimental ablation of the pituitary does not impair prenatal growth (reviewed by Fowden, 1995). In most mouse strains, the growth of the

141

GH-deficient spontaneous mutants Snell (dwarf, *dw*), Ames (*df*), and little (*lit*) is indistinguishable from that of wild-type littermates for approximately the first 2 weeks after birth, at which time growth retardation begins to be manifested. Eventually, the Snell dwarfs (lacking both GH and thyroid-stimulating hormone) reach a relative size of $\sim 30\%N$, whereas the Ames and *lit* mice (possessing residual GH activity) become $\sim 50\%N$ in weight. These dwarf mice (for reviews, see Watkins-Chow and Camper, 1998; Kioussi *et al.,* 1999) carry, respectively, missense mutations of the genes *Pit1* (encoding a transactivator essential for the expression of GH, prolactin, and thyroid-stimulating hormone β subunit), *Prop1* (encoding a trans-activator essential for expression of *Pit1* and expansion of Pit1-controlled pituitary cell lineages), and *Ghrhr* (encoding the receptor of the GH-releasing hormone). Although invaluable for a variety of studies, these spontaneous mouse dwarfs are not ideal models to address questions about the GH/IGF axis in postnatal growth, as they exhibit combined pituitary hormone deficiencies and/or possess some residual GH activity. Similar drawbacks exist with studies involving hypophysectomy, which removes not only GH but also other hormones known to affect growth (especially thyroid hormone regulators; see Williams *et al.,* 1998). Thus, to explore the relationship between GH and IGF1 in growth control, we used an alternate genetic approach based on the following considerations.

The original "somatomedin hypothesis" (Salmon and Daughaday, 1957; for a review, see Daughaday, 1989; Scanes and Daughaday, 1995) was proposed on the basis of results demonstrating that GH (somatotropin) stimulated sulfate incorporation into cartilage indirectly through a serum factor (somatomedin; mediator of the effects of somatotropin). In its more general form, the hypothesis posited that GH stimulates the hepatic production of circulating somatomedin (i.e., IGF1), which then mediates the hormonal effects on target tissues. However, despite evidence for an apparent endocrine role of the plasma IGF1 (reviewed by Zapf, 1998), its involvement in growth control was recently disputed on the basis of results with a conditional *Igf1* gene knockout in mice (Sjögren *et al.,* 1999; Yakar *et al.,* 1999; see Results and Discussion). Moreover, direct effects of GH on cartilage, apparently mediated by locally produced and not by circulating IGF1 (Isaksson *et al.,* 1982; Nilsson *et al.,* 1986; Schlechter *et al.,* 1986; reviewed by Isaksson *et al.,* 1987; Ohlsson *et al.,* 1998), remained undetectable in the pioneering experiments (Salmon and Daughaday, 1957) for technical reasons (Salmon and Burkhalter, 1997). Finally, in regard to IGF1-independent action of GH, a "dual effector theory" was proposed (Green *et al.,* 1985), according to which GH stimulates the differentiation of progenitor cells, making them responsive to IGF1.

Although the original version of the somatomedin hypothesis is not tenable, the important issues pertaining to the exact relationship between GH and IGF1 and the relative magnitudes of their contributions to growth have not been resolved yet. In fact, in regard to bone development, the picture is still quite unclear, while similar confusion exists when other IGF1 or GH target tissues are considered.

To investigate genetically the relationship between GH and IGF1 in postnatal growth, we sought to generate double-mutant mice lacking the actions of both GH and IGF1 and compare their phenotype with the phenotypes of the respective single mutants. For this purpose, we used available *Igf1* mutant mice (Liu *et al.,* 1993) and generated mutants lacking GH action by knocking out the gene encoding GHR. While this work was in progress, a report appeared also describing targeted inactivation of the *Ghr* gene by a different strategy (deletion of the 3' portion of exon 4 and part of the downstream intron; Zhou *et al.,* 1997). Mice lacking GHR function are potential models of Laron-type dwarfism, a growth-retardation disorder resulting from mutations in the human *Ghr* gene (see Rosenfeld *et al.,* 1994; Laron, 1999; Kopchick and Laron, 1999).

MATERIALS AND METHODS

Ghr Gene Targeting and Breeding of Mutants

To isolate mouse clones carrying portions of the *Ghr* gene, we screened a genomic λ phage library from strain 129/Sv with a partial cDNA probe synthesized by RT-PCR using mouse liver RNA and the primers 5'-TCCACCCATTGGCCTCAACTGGA-CTT-3' (forward; in exon 6) and 5'-TGGCGGATCCTCTGAA-GCTGGTGAT-3' (reverse; in exon 8a; Edens *et al.,* 1994). A targeting vector was then constructed from subcloned genomic fragments in several steps. For selection of targeted clones, neomycin (*neo*) and thymidine kinase (*tk*) gene cassettes placed in transcriptional orientation opposite to that of the endogenous locus were included in the construct (Fig. 1a). The final product (cloned into pBluescript SK(+); Stratagene) consisted of a 5' genomic fragment containing exon 6 (9.6 kb), from a *Not*I site (initially in the phage polylinker) to an *Xba*I site, the *neo* cassette (1.7 kb; *Xba*I to *Xba*I), a downstream *Ghr* genomic fragment (2.4 kb; from an *Xba*I site to a *Sal*I site initially present in the phage polylinker), and the *tk* cassette (1.85 kb; *Sal*I to *Xho*I). Thus, a 4-kb *Xba*I–*Xba*I *Ghr* genomic fragment containing exons 7, 8a, and 8 was replaced with the *neo* cassette.

Linearized targeting vector DNA was introduced by electroporation into 129/Sv ES cells (CCE-33) and, after drug selection, DNA of resistant clones was analyzed by Southern blotting (Figs. 1a and 1b). In addition, a *neo* probe was used to demonstrate that single-copy integration had occurred in the targeted ES cells. To generate chimeras, cells of a targeted clone were injected into host blastocysts of C57BL/6J like mice that were transferred into uteri of pseudopregnant females.

Male chimeras were mated with C57BL/6J females and F1 heterozygous progeny were intercrossed. To generate *Ghr*(+/−)/*Igf1*(+/−) double heterozygotes, we crossed *Ghr*(+/−) mutants (129 Sv/C57BL/6J) with heterozygous mice (MF1/DBA) carrying a targeted mutation of the *Igf1* gene (Liu *et al.,* 1993; Baker *et al.,* 1993, 1996). The particular genetic background of *Igf1* mutants was chosen on the basis of empirical observations, to increase the frequency of surviving nullizygotes obtained in subsequent crosses (there is a strain-dependent, high incidence of neonatal lethality

among *Igf1* nullizygotes; Liu *et al.,* 1993). The *Ghr/Igf1* double heterozygotes and the progeny derived from their intercrosses, including double nullizygotes, carried components of four strain backgrounds in variable mixtures. Double null mutants were also obtained by intercrossing *Ghr*(−/−)/*Igf1*(+/−) parents generated from double heterozygote intercrosses (double nullizygotes cannot be intercrossed because both sexes of *Igf1* null survivors are infertile; Baker *et al.,* 1996). Mice were genotyped for the *Ghr* mutation as described above for targeted ES cells and for the *Igf1* mutation as described previously (Liu *et al.,* 1993).

RNA Analysis

Northern blots of total liver RNA (20 μg) from wild-type, *Ghr*(+/−) and *Ghr*(−/−) mice were hybridized with a 586-bp probe representing a mouse *Ghr* cDNA fragment (exons 1 through 6) obtained by RT-PCR using the primers 5′-CAGGTCTTCTTAAC-CTTGGCACTGGC-3′ (forward) and 5′-AAGTCCAGTTGAGG-CCAATGGGTGGA-3′ (reverse).

Semiquantitative RT-PCR assays of steady-state *Igf1* mRNA using β-actin mRNA as a standard were performed in duplicate using the following primer pairs (the members of each pair represent sequences in different exons of the respective genes, to avoid amplification of genomic DNA potentially contaminating the samples): 5′-ACCAAAATGACCGCACCTGC-3′ (*Igf1* forward), 5′-AACACTCATCCACAATGCCTGTC-3′ (*Igf1* reverse), 5′-GAC-AACGGCTCCGGCATGTGCAAAG-3′ (actin forward), and 5′-TTCACGGTTGGCCTTAGGGTTCAGGG-3′ (actin reverse). The conditions for linear *Igf1* amplification (midlog phase of PCR) were denaturation at 94°C (15 s), annealing at 57°C (15 s), and extension at 60°C (30 s). The number of cycles varied between samples (liver 11; kidney, ovary, and testis 15; and brain, heart, and lung 18). Except for the annealing temperature (70°C), the conditions for actin amplification (11 cycles) were the same. For each organ, the *Igf1* and β-actin reaction products were mixed, fractionated on a 3% NuSieve agarose gel, and transferred onto nylon membranes. In this Southern analysis, the respective PCR products were used as hybridization probes and the signals were quantitated using a PhosphorImager (Molecular Dynamics). From these readings, ratios of *Igf1* and β-actin signal intensities were calculated (normalization) and then compared between mutant and wild-type specimens. Statistically significant differences in pairwise comparisons of these and other data were evaluated using Student's *t* test at a rejection level of 5%.

Protein Analysis

Protein amounts were determined by BCA assays (Pierce). Western analyses were performed as described (Eggenschwiler *et al.,* 1997). For analysis of GHR by Western blotting, we used hepatic microsomal protein extracts (Smith and Talamantes, 1987) from 17-day-pregnant *Ghr*(−/−) and control females. The primary antibody (As 2941) against the intracellular domain of the mouse GHR was a gift from Dr. G. P. Frick (Frick *et al.,* 1994). Attempts to visualize a truncated protein in the mutants by Western analysis using a commercially available antibody against the N-terminal domain of GHR/GHBP (Anawa, Switzerland) were unsuccessful. For Western blotting or RIA, serum IGF1 was partially purified by acid–ethanol cryoprecipitation (Breier *et al.,* 1991) and detected with an anti-human IGF1 monoclonal antibody (R&D Systems). Radioimmunoassays were performed using a kit (Nichols Institute). The lowest of three serum dilutions used in these RIA

measurements was 1:50 (higher serum concentrations generated nonparallel competition curves and high background even with negative control sera from *Igf1* null mice). The primary antibody used for GH detection was provided by Dr. A. F. Parlow and the National Hormone and Pituitary Program (Baltimore, MD).

Bone Histology and Morphometry

Tibiae and femora from animals perfused with buffered formalin were decalcified for 3–4 days in Cal-EX II solution (Sigma); washed for 24 h at 4°C in a solution containing 0.25 M sucrose, 0.2 M glycine, and 0.1 M sodium phosphate buffer (pH 7.3); dehydrated; cleared with toluene; and embedded in paraffin. Paraffin blocks were sectioned at 6–8 μm and stained with hematoxylin and eosin.

Measurements were taken on cleaned bones from perfused animals with a dial caliper (Scienceware). The measurement of epiphyseal width corresponds to the widest dimension, while that of diaphyseal width is the average of two determinations per tibia, above and below the point where the fibula joins the diaphysis distally.

Morphometry was performed on photographs of longitudinal sections (close to the midline of the bone) taken with a Nikon digital camera. The total height of the growth plate (GP) was considered the distance between the two chondrosseous junctions: proximal (border between the secondary ossification center and the chondrocytes of the resting zone; see Results and Discussion) and distal (border between the hypertrophic zone and the beginning of spicules of trabecular bone). To measure the heights of the proliferative and hypertrophic zones (PZ and HZ), their borders were delineated on the basis of morphological criteria. Thus, the proliferative zone was measured from the top of the columns of chondrocytes to the border of the hypertrophic zone that corresponds approximately to the point where the ratio of cell width to cell height reaches ~2 (see Vanky *et al.,* 1998). The distance between this point and the distal chondrosseous junction was considered the height of the hypertrophic zone. We defined the height of each resting zone (RZ; see Results and Discussion) by subtraction: RZ = GP − (PZ + HZ).

BrdU Labeling

Labeling of chondrocytes with bromodeoxyuridine (BrdU) was performed as described (Eggenschwiler *et al.,* 1997). The animals were sacrificed 1 h after injection of BrdU at postnatal day 22 (p22). Stained and unstained cells were counted in one rectangle per section, using four sections close to the midline per animal, and four animals per phenotype (16 determinations per growth plate of each phenotype). The same size of rectangle, always positioned within the zone of proliferating chondrocytes, was used for all sections regardless of phenotype. Values were expressed as percentages of the total number of cells that were BrdU positive. The average and the standard error were calculated from the means of the four animals for each genotype.

In Situ Hybridization

Nonisotopic *in situ* hybridization with digoxigenin-labeled probes was performed on dewaxed paraffin sections. After rehydration, we followed a procedure described previously for fixed frozen sections (Schaeren-Wiemer and Gerfin-Moser, 1993). For detection of *Igf1* transcripts we used a full-length *Igf1* cDNA (GenBank Accession No. AI314558). The probe to examine *Ghr* expression

was the same as that described above for Northern analysis. The hybridization signal was amplified with the TSA Biotin System (NEN). The probes used for detection of collagen mRNAs were described previously (Lee *et al.,* 1994).

Growth Analysis

Despite frequent weight measurements, in the dataset of derived values, not all mice were measured on each and every day, while the times of determinations often differed between litters. For these reasons, postnatal growth curves of wild-type and mutant mice were constructed and fitted as follows: First, to determine average absolute growth rates (weight changes per day), we subjected the entire set of data for each phenotype to statistical analysis using maximum-likelihood methods (described in detail at http://www.columbia.edu/~ae4/GHR_IGF1_AP.html). The plots of these initial growth rates have rather jagged forms, but when they are transformed to conventional growth curves (plots of cumulative weight versus age), the estimates follow paths that are quite smooth (i.e., fluctuations of values are only a minor, not a prominent, feature). To rederive rate curves that would also be smooth, we used a two-step procedure based on the consideration that cumulative postnatal growth curves are best fitted with a logistic equation $W = A/1 + \exp[-b(t - c)]$, where W and A are the weight at time t and the asymptotic weight, respectively, while b and c are constants. A second consideration was that, for the period of displayed observations (100 postnatal days), growth is clearly triphasic. Thus, between an early neonatal growth period (~2 weeks) and a growth spurt after weaning, there is a period of considerable decline in growth rate. However, the growth of wild-type mice during this intermediate period simply slows down, whereas in the mutants described here growth becomes negative. On the basis of these features, the weight data were fitted simultaneously using a computer program (SigmaPlot) by summation of three logistic functions with different sets of A, b, and c values (Koops, 1986; Koops *et al.,* 1987). Moreover, we found empirically that a faster and better fit accommodating the data of negative growth is achieved if a negative sign is assigned to the second of the three equations, giving positive values to the other two. (In contrast to the mutants, the final fit of wild-type data was insensitive to the sign of the second equation.) From each fit, curves of predicted absolute growth rates (dW/dt) were derived (same as the initial rate curves, but smooth) by subtracting the value of cumulative weight at each day (W_i) from that estimated for the previous day (W_{i-1}). Furthermore, for even more sensitive comparisons, each absolute growth rate was transformed to a specific growth rate [i.e., growth rate per unit size; (dW/dt) $\times$ ($1/W$)] using weight values for normalization: $(W_i - W_{i-1})/[\frac{1}{2} \times (W_i + W_{i-1})]$.

Organ weights were determined as described (Eggenschwiler *et al.,* 1997). Body lengths (from the tip of the nose to the base of the tail) were measured on anesthetized animals stretched on top of a ruler.

RESULTS AND DISCUSSION

Analysis of Ghr(−/−) Mutants

Targeted disruption of the mouse Ghr gene. To generate mutants lacking GH functions, as required by our experimental design (see Introduction), we chose to target *Ghr* rather than the *Gh* gene itself, so that we could

ascertain at the same time whether the embryonic expression of GHR plays some indispensable physiological role (it turned out that it does not).

The mouse gene encoding GHR is large (>90 kb) and contains more than 2 alternate 5′ noncoding exons and 11 coding exons, the last 2 of which (9 and 10) encode the intracellular domain of the receptor (Moffat *et al.,* 1999). The same gene also encodes GH-binding protein (GHBP), which corresponds to the extracellular domain of GHR and is found in the circulation associated with GH. In rodents, but not in all examined species, the *Ghbp* (~1.2 kb) and *Ghr* (~4.2 kb) mRNAs are generated, respectively, by alternate splicing of exon 7 either to exon 8a (encoding the C-terminal domain of GHBP and the 3′ noncoding region of the corresponding mRNA) or to exon 8 (encoding the transmembrane domain of GHR).

To generate a null mutation of the *Ghr* gene, we used a targeting vector that would replace exons 7, 8a, and 8 with a *neo* cassette (Fig. 1a). The targeted allele (Figs. 1a and 1b) was designated Ghr^{ex7-8}. $Ghr(-/-)$ mice were obtained at the expected Mendelian ratios. They exhibited postnatal growth retardation (see below), but they were viable and fertile, although, as previously described for a similar mutation (Zhou *et al.,* 1997), the sexual maturation of females was delayed and the litter sizes were small.

To demonstrate that Ghr^{ex7-8} was a null allele, we first performed Northern analysis of total liver RNA using a cDNA probe (exons 1–6) able to recognize both the *Ghr* and the *Ghbp* mRNA species (Fig. 1c). The results showed that the 1.2-kb mRNA species encoding GHBP was not present in $Ghr(-/-)$ mutants, as expected from the deletion of exon 8a containing the *Ghbp* mRNA polyadenylation signal. On the other hand, a transcript with a size similar to that of wild-type *Ghr* mRNA (4.2 kb) was still present in the mutants, but at a significantly reduced level (Fig. 1c). This mutant transcript was predicted to lack the short exons 7 and 8 (0.26 kb), but the small size difference from wild-type could not be monitored convincingly by a shift in electrophoretic mobility. Thus, after RT-PCR using primers in exons 6 and 10, we sequenced a region of the mutant mRNA and demonstrated directly that splicing had occurred between exons 6 and 9, resulting in a predicted frame shift and the appearance of a stop codon at the beginning of exon 9 (Fig. 1d). Not unexpectedly, therefore, the amount of the mutant *Ghr* mRNA was significantly reduced in comparison with the controls, considering that a surveillance mechanism is in operation, which detects and degrades abnormal mRNAs carrying nonsense codons that can lead to premature translational termination (Frischmeyer and Dietz, 1999).

On the basis of the mutant mRNA analysis, we inferred that any truncated GHR synthesized in $Ghr(-/-)$ embryos would lack an intracellular domain. Consistent with this expectation, Western analysis demonstrated that an antibody against the intracellular GHR domain failed to recognize GHR in preparations of hepatic microsomes from $Ghr(-/-)$ mutants, in contrast to wild-type controls (Fig.

a

Ghr gene

targeting vector

targeted locus

1 kb

b

HindIII   EcoRV
T   NT   T   NT

◄8.7 kb
◄8.4 kb

6.6 kb►

5.2 kb►

c

Ghr Ghr Ghr
+/+ +/- -/-

4.2 kb►   Ghr

1.2 kb►   Ghbp

Gapd

d

EXON 6

TCCACCCATTGGCCTCAACTGGACTT

TCCACCCATTGGCCTCAACTGGACTTTACTAAACATTAGTTTGACCGGGATTCGTGGAGACATCCAAGTGAGTTGGCAACCACCACCCAATGCAGATGTTCTGAAGGGATGGATAATTCTGGAGTATGAAATTC

AGTACAAAGAAGTAAATGAATCAAAATGGAAAGTG ▼ EXON 9
GAT**TAA**GATGCTGATTTTACCCCCAGTCCCAGTTCCAAAGATTAAAGGGATTGATCCAGATCTTCTCAA ▼ EXON 10
       STOP
GGAAGGGAAGTTGGAGGAGGTGA
GTT CCTTCCCTTCAACCTCCTCCACT

e

Ghr   Ghr
+/+   -/-

~110 kD►

f

Igf1   Igf1   wt   wt   Ghr   Ghr
-/-   -/-   -/-   -/-

serum ► 50 µl 50 µl 5 µl   5 µl   50 µl 50 µl
rhIGF1 ► 1 ng   -   -   -   -   -

~7.5 kD►

g

wt   wt+GH   Ghr   Igf1
              -/-   -/-

~23 kD◄

h

wt   Ghr(-/-)

Liver   A
                               I

Lung   A
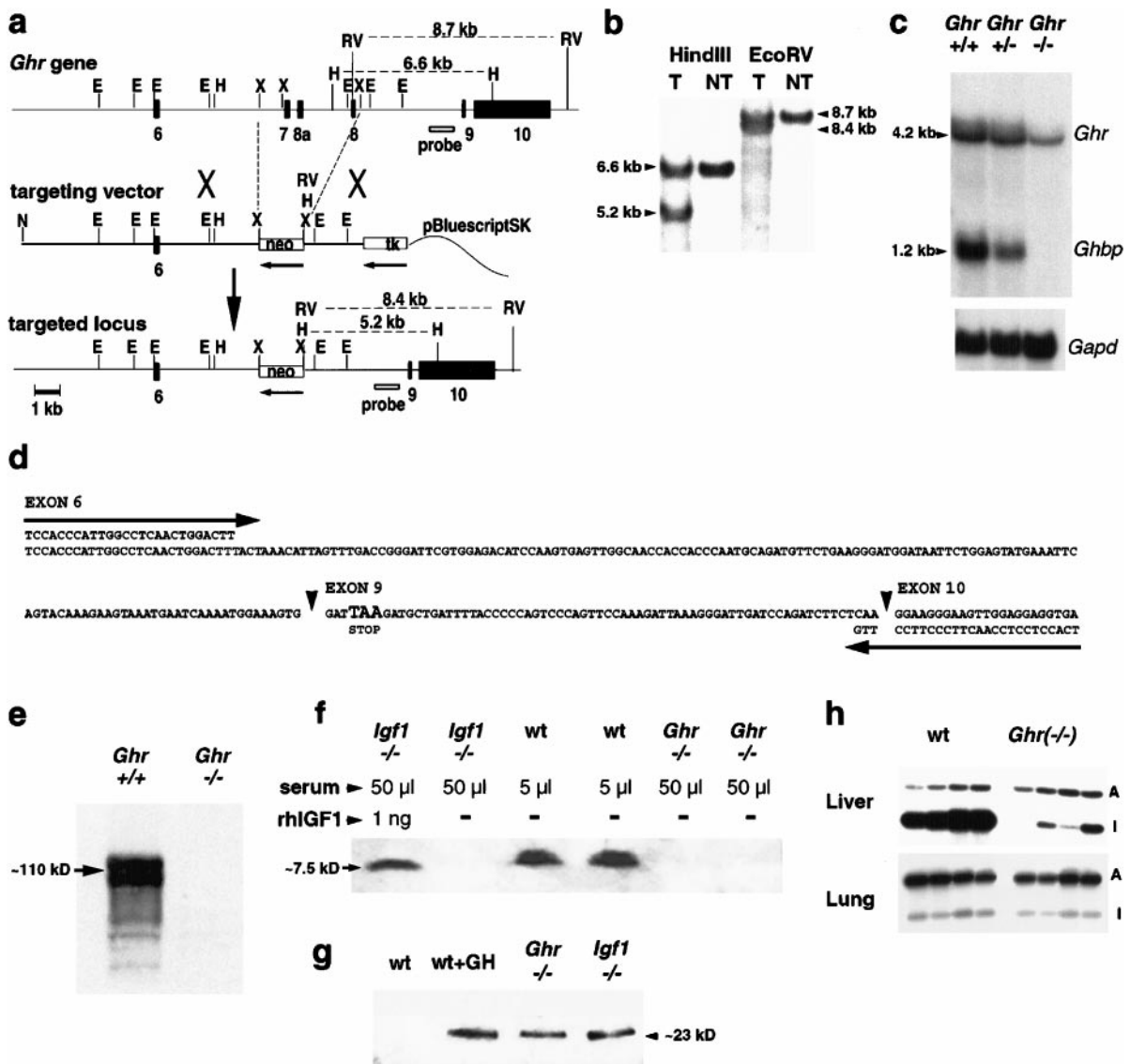   I

FIG. 1. Targeting of the mouse *Ghr* locus and molecular analyses of mutants. (a) The restriction map in the region of exons 6–10 (black rectangles) of the *Ghr/Ghbp* gene (top), the targeting construct (middle) used for gene disruption by homologous recombination (denoted by large X symbols), and the structure of the derived (arrow) targeted allele (bottom) are shown. The transcriptional orientations of the *neo* cassette (replacing the deleted exons 7, 8a, and 8) and of the *tk* cassette are indicated with arrows. The wavy line represents plasmid vector sequence. N indicates a *Not*I site used to linearize the replacement vector. Other restriction sites are *Eco*RI (E), *Hin*dIII (H), *Xba*I (X), and *Eco*RV (RV). The position of the probe (a 1.0-kb *Sau*3A fragment located in the *Ghr* locus downstream of the 3′ region of homology present in the vector) that was used for Southern analyses of ES cell clones and mice is indicated, and the sizes (in kb) of the endogenous and targeted *Hin*dIII and *Eco*RV genomic DNA fragments recognized by this probe are shown. (b) Examples of Southern blots of *Hin*dIII- and *Eco*RV-digested genomic DNA from targeted (T) and nontargeted (NT) ES cell clones hybridized with the probe shown in (a). (c) Northern analysis of liver RNA isolated at p60 from wild-type (+/+), heterozygous (+/−), and nullizygous (−/−) *Ghr* mice. The membrane was hybridized with a *Ghr/Ghbp* cDNA probe (exons 1–6) and then stripped and rehybridized with a mouse glyceraldehyde-3-phosphate dehydrogenase (*Gapd*) cDNA probe (detecting a 1.2-kb transcript), to provide a loading control. (d) Results of DNA sequencing of cloned RT-PCR products using liver *Ghr*(−/−) mutant mRNA template and the indicated primers (arrows). The sequence demonstrates that, in the mRNA from the mutated locus, splicing has occurred between exon 6 and exon 9, resulting in the generation of a stop codon (TAA; bold letters) at the beginning of exon 9. (e) Western analysis of protein extracts from hepatic microsomal membranes isolated at p60 from wild-type (+/+) mice and *Ghr* nullizygotes (−/−) using an antiserum against the intracellular domain of the ~110-kDa GHR protein (seen as a doublet). (f) Western analysis of acid–ethanol serum extracts from p180 wild-type mice (wt), *Igf* nullizygotes (negative control), and *Ghr* nullizygotes using an antibody recognizing IGF1 (~7.5 kDa). The amount of protein loaded on each lane was extracted from the indicated serum volume (in µl). Human recombinant IGF1 (1 ng) was added to a sample of serum from an *Igf1*(−/−) mutant as a positive control. (g) Western analysis of unfractionated sera (5 µl per lane) from mice such as those described in (f) using an antibody that detects GH (~23 kDa). The amount of GH in wild-type serum (first lane) was below the detection limit of this assay. Purified mouse pituitary GH (1 ng) was added to a sample of wild-type serum (second lane) as a positive control. (h) Examples of semiquantitative RT-PCR analysis of steady-state *Igf1* mRNA (band I) in the liver and lungs of p180 wild-type (wt) and *Ghr* nullizygous mice (display of amplification products by Southern blotting; see Materials and Methods). Four animals (two male and two female) of each genotype were examined. Amplification of *β*-actin mRNA (band A) was used as a standard.

145

1e). Attempts to detect a truncated, soluble form of GHR resembling GHBP were unsuccessful (see Materials and Methods). However, any role that this presumptive GHBP-like molecule could potentially play in the mutants would be inconsequential (it would affect only the GH ligand that cannot function in the absence of GHR signaling).

IGF1 and GH assays in Ghr(−/−) mutants. Because circulating IGF1 is under GH control (reviewed by Scanes and Daughaday, 1995), we measured serum IGF1 levels in adult (~6 months of age) $Ghr(-/-)$ mutant and wild-type mice by a radioimmunoassay (RIA), using as negative controls sera from *Igf1* nullizygotes. The results demonstrated that the IGF1 concentration was 194 ± 9 ng/ml in normal sera, whereas in $Igf1(-/-)$ and $Ghr(-/-)$ mutant sera it was below the detection limit of the assay (0.4 ng/ml). Considering that the lowest of three serum dilutions used in these measurements was 1:50 (see Materials and Methods), we estimated that the concentration of IGF1 in $Ghr(-/-)$ mutant serum could not exceed ~10% of the normal value $[(0.4 \times 50)/194]$.

In addition, independent results were obtained by Western analysis using a different antibody (Fig. 1f). Application of this technique, which is more sensitive than RIA and can detect at least 0.1 ng of IGF1 per lane, indicated that the serum level of IGF1 in $Ghr(-/-)$ mutants was closer to ~0.2% of normal. As shown in an example of such assays (Fig. 1f), using as a positive control recombinant human IGF1 and as a negative control serum from *Igf1* null mice, IGF1 peptide was undetectable in mutants lacking GHR, although the amount of acid–ethanol-extractable proteins from mutant sera that was electrophoresed was 10-fold higher than that from wild-type specimens (50 vs 5 μl). Nevertheless, an extremely faint IGF1 signal (barely visible above background; ~0.1 ng) was detected on occasion in other assays (not shown) by loading on the gel protein extracted from 250 μl of mutant serum (0.1 ng/250 μl = 0.4 ng/ml; $0.4/194 \approx 0.2\%$ of normal). The level of serum IGF1 in a similar *Ghr* knockout was reportedly 7–10% of normal (Zhou *et al.,* 1997; Sjögren *et al.,* 2000; Coschigano *et al.,* 2000) or undetectable (Chandrashekar *et al.,* 1999).

In mice, the physiological mode of GH secretion is pulsatile in both sexes, although the interval between pulses is longer in males (~2.5 h vs <1 h in females; MacLeod *et al.,* 1991). Therefore, single measurements of circulating GH, although often reported, are not very informative. Nevertheless, to demonstrate that a major negative feedback regulating pituitary GH secretion that is exerted at both the hypothalamic and the pituitary levels by the circulating IGF1 (Berelowitz *et al.,* 1981; Tannembaum *et al.,* 1983; Yamashita and Melmed, 1986) was ablated in both *Ghr* and *Igf1* null mutants, we assayed GH levels in serum by Western blotting (Fig. 1g), but did not attempt to derive accurate quantitative results. Using pituitary GH both as a positive control and as a size marker, we showed that GH protein was undetectable in 5 μl of serum from wild-type mice (the maximum amount that could be loaded on a lane), whereas serum from $Ghr(-/-)$ or $Igf1(-/-)$ mice (5

TABLE 1

Relative Levels of *Igf1* Transcripts

Tissue	W	G	Δ [a]
Brain	100 ± 5.0	108.7 ± 6.3	−
Lung	100 ± 24.2	87.8 ± 4.3	−
Heart	100 ± 19.7	99.5 ± 20.9	−
Liver	100 ± 13.2	2.2 ± 1.2	+
Kidney	100 ± 11.2	59.7 ± 6.6	+
Testis	100 ± 13.5	92.6 ± 0.5	−
Ovary	100 ± 13.4	29.2 ± 4.3	+
Uterus	100 ± 8.7	77.6 ± 5.3	−

[a] The presence (+) or absence (−) of a statistically significant difference (Δ) between wild-type animals (*W*) and $Ghr(-/-)$ mutants (*G*) is indicated (Student's *t* test; $P < 0.05$). Mean values $\pm$ SE (expressed as percentages of control levels after normalization; see Materials and Methods) were calculated from measurements of four specimens per tissue (two from male and two from female animals), except for reproductive tissues (two specimens). The mean $\pm$ SE (standard error) shown in each case was calculated by dividing each of the values by the average of the corresponding wild-type signal (considered 100%) and averaging again the derived set of percentage values.

μl) yielded a strong signal indicating high levels of circulating GH.

GH-dependent and GH-independent Igf1 expression. To assess the steady-state level of *Igf1* transcripts in various tissues, we performed semiquantitative RT-PCR analysis using RNA from wild-type and $Ghr(-/-)$ specimens of liver, heart, lung, kidney, brain, and reproductive organs (Table 1; examples of the assays are shown in Fig. 1h).

As expected from previous results with *lit* mutant mice (Mathews *et al.,* 1986; Sugisaki *et al.,* 1993), which maintain only ~10% of the normal GH level (Cheng *et al.,* 1983), we detected a dramatic reduction in the level of *Igf1* expression in $Ghr(-/-)$ mutant liver (~1–2% of the normal value). It is known that GH increases hepatic *Igf1* gene expression at the transcriptional level, as demonstrated by run-on assays (Mathews *et al.,* 1986).

The practically complete dependence of liver *Igf1* transcripts on GH action appears to be unique. In all other examined tissues, *Igf1* expression, if not GH-insensitive, is only partially dependent on GH, as observed in the ovary and, in agreement with previous reports (Mathews *et al.,* 1986; Sugisaki *et al.,* 1993), in the kidney (Table 1). In other major organs (heart, lung, testis, uterus; Table 1), *Igf1* expression was found to be GH-independent. The same observation was made in the spleen (Mathews *et al.,* 1986) and also in the brain (Table 1 and Sugisaki *et al.,* 1993). Thus, a minor negative effect of GH deficiency on brain *Igf1* reported previously (Mathews *et al.,* 1986) was not confirmed.

GH-independent IGF1 expression was also demonstrated in some rat tissues, including for example testis (Spiteri-Grech *et al.,* 1991) and skin (Lemmey *et al.,* 1997), whereas
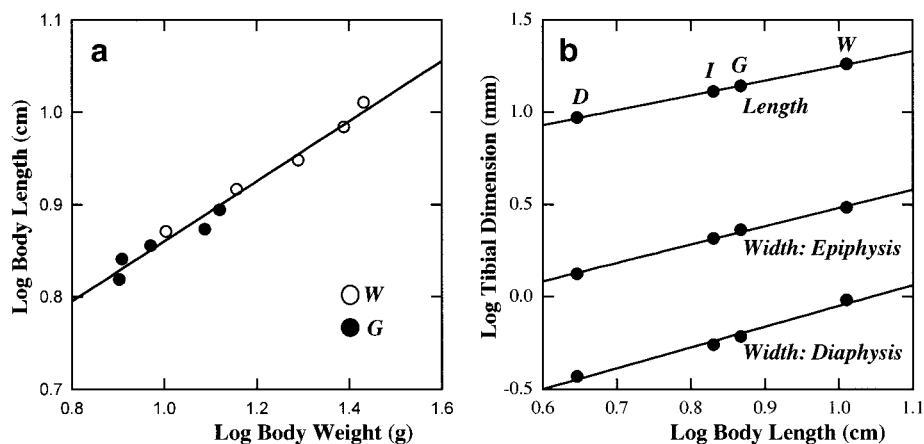
FIG. 2. Allometric plots. (a) Log–log plot and first-order regression of the body lengths of wild-type (*W*) and *Ghr*(−/−) mutant (*G*) mice vs corresponding weights determined at 18, 25, 31, 45, and 60 days of age. For further details, see text. (b) Log–log plots of the length (T_L) and of the epiphyseal (T_E) and diaphyseal (T_D) widths of the tibia vs body length (B_L) at p130 (see data in Table 3). The results of the corresponding regression analyses were $T_L = 2.8B_L^{0.8}$, $T_E = 0.3B_L^{1.0}$, and $T_D = 0.07B_L^{1.1}$ ($r > 0.99$). A slope of 1.0 or close to 1.0 in all cases indicates an isometric relationship.

other results were either conflicting between reports or in disagreement with the mouse data (see Murphy *et al.,* 1987; Roberts *et al.,* 1987; Hynes *et al.,* 1987; Butler *et al.,* 1994).

According to our evidence, as a direct consequence of ablation of GH action in *Ghr* nullizygotes, there is absence of *Igf1* transcripts in the liver correlating with a lack of immunoreactive IGF1 in serum. Although this correlation does not prove that hepatocytes are the sole source of IGF1 present in the circulation, it poses the following severe restriction on the occasionally postulated, but experimentally unsupported and unlikely, extrahepatic origin of circulating IGF1. If in addition to the liver another source contributing to serum IGF1 exists, expression of *Igf1* in this particular tissue should be GH-dependent.

Scaling. The growth retardation of *Ghr*(−/−) mutants is described in a later section. However, because weight does not necessarily reflect linear growth, we performed a limited allometric analysis of the relationship between body lengths (BL) and body weights (BW) measured at different developmental ages. For this purpose, we used the allometric scaling equation $y = a \cdot x^b$ in its logarithmic form $\log y = \log a + b \log x$, where y is BL, x is BW, b is the slope of the regression line, and a is the y intercept (see Shea *et al.,* 1987). In a length vs weight comparison, simple extension of the regression line of a dwarf mutant by the corresponding line of the wild-type control indicates an isometric relationship (common trajectory of relative growth) with a predicted slope of 0.33 (lack of allometric scaling and no change in proportion). This was almost exactly what our analysis showed (Fig. 2a), as the results of regression analysis for the wild-type and *Ghr*(−/−) mice were BL = 3.42 · BW$^{0.326}$ (coefficient of correlation $r = 0.99$), indicating that the mutants are normally proportioned. Interestingly, in a similar comparison between wild-type

and transgenic mice overexpressing GH, it was found that the nose-to-rump length exhibited an isometric relationship to body weight in both groups of animals (Shea *et al.,* 1987).

We also observed that the weights of major organs determined at 1 and 3 months of age were reduced in the *Ghr*(−/−) mutants proportionate to body weights in comparison with wild-type controls, with the exception of the brain and kidney and also the spleen in the older animals (Table 2). The kidney and spleen were disproportionately reduced in size, whereas the brain/body weight ratio was relatively increased by 70% in p30 mutants. Most likely, this difference is due to the fact that brain growth is practically completed by the time GH action commences in mice (see Winick and Grant, 1968; Bishop and Wahlsten, 1999). Thus, although the normal brain to body weight ratio becomes relatively smaller as growth proceeds (negatively allometric relationship), this ratio is higher in *Ghr*(−/−) mutants in comparison with wild-type controls because of their growth retardation (smaller denominator).

Despite deviations from isometric scaling in particular organs, the dwarfism of mice lacking GHR is almost ateliotic (proportionate). This observation, in conjunction with the previous conclusion that the GH control of IGF1 expression varies between extrahepatic tissues and may be partial or absent, suggests strongly that the magnitude of this dependence, wherever it occurs, is small. Otherwise, significantly negative allometric relationships with different severities of impact between organs would have been observed.

Comparison of Growth Retardation Phenotypes

Genetic crosses and growth curves. To investigate genetically the relationship between GH and IGF1 in postna-

TABLE 2

Comparison of Organ Weights between Wild-Type and *Ghr*(−/−) Mice

	p30					p90				
	Weight (mg)		% Body weight (% of control)[a]			Weight (mg)		% Body weight (% of control)		
Organ	*W*	*G*	*W*	*G*	Δ	*W*	*G*	*W*	*G*	Δ
				(A) Males						
Brain	405.4 ± 12.0	375.6 ± 9.1	2.00 ± 0.13 (100 ± 6.99)	3.46 ± 0.15 (170 ± 7.2)	+	453.5 ± 5.9	361.8 ± 10.4	1.59 ± 0.04 (100 ± 2.8)	2.13 ± 0.15 (133.9 ± 9.3)	+
Thymus	86.3 ± 4.5	54.2 ± 5.9	0.42 ± 0.04 (100 ± 8.8)	0.49 ± 0.03 (116.2 ± 6.4)	−	49.4 ± 4.9	33.4 ± 4.6	0.17 ± 0.01 (100 ± 7.3)	0.19 ± 0.01 (112.7 ± 8.3)	−
Heart	103.3 ± 4.5	61.2 ± 3.5	0.50 ± 0.01 (100 ± 2.9)	0.56 ± 0.01 (112.6 ± 2.5)	−	121.6 ± 3.2	59.1 ± 5.3	0.43 ± 0.01 (100 ± 2.3)	0.35 ± 0.03 (80.4 ± 7.5)	−
Lungs	278.5 ± 19.4	154.3 ± 16.4	1.34 ± 0.06 (100 ± 4.5)	1.41 ± 0.13 (105.3 ± 9.5)	−	239.5 ± 15.2	152.4 ± 19	0.84 ± 0.05 (100 ± 5.6)	0.87 ± 0.05 (104.2 ± 5.8)	−
Liver	945.3 ± 35.9	503.9 ± 74.5	4.59 ± 0.29 (100 ± 6.3)	4.57 ± 0.51 (99.6 ± 11.2)	−	1234.6 ± 144	565.4 ± 61.6	4.37 ± 0.63 (100 ± 14.5)	3.28 ± 0.29 (75.1 ± 6.7)	−
Spleen	81.1 ± 3.8	36.1 ± 6.2	0.39 ± 0.02 (100 ± 6.2)	0.33 ± 0.04 (83.6 ± 10.8)	−	61.9 ± 3.4	24.8 ± 2.2	0.22 ± 0.01 (100 ± 6.7)	0.14 ± 0.01 (65.1 ± 2.3)	+
Kidneys	317.0 ± 18.2	134.1 ± 10.1	1.52 ± 0.01 (100 ± 2.4)	1.23 ± 0.06 (80.7 ± 3.8)	+	434.8 ± 28.8	174.7 ± 12.3	1.52 ± 0.06 (100 ± 4.3)	1.02 ± 0.07 (67.2 ± 4.8)	+
Testes	154.6 ± 10.2	71.3 ± 9.9	0.75 ± 0.04 (100 ± 5.6)	0.66 ± 0.1 (87.7 ± 13)	−	229.9 ± 12.9	118.1 ± 5.4	0.8 ± 0.02 (100 ± 2.8)	0.7 ± 0.06 (99.4 ± 8.2)	−
Body (g)	20.8 ± 1.1	10.9 ± 0.6				28.6 ± 1.1	17.3 ± 1.4			
n	6	4				4	4			
				(B) Females						
Brain	406.9 ± 17.8	387.3 ± 7.8	2.45 ± 0.11 (100 ± 4.4)	4.00 ± 0.34 (163.2 ± 14)	+	422.9 ± 18.4	391.9 ± 16.0	1.84 ± 0.02 (100 ± 1.2)	2.57 ± 0.03 (139.9 ± 15)	+
Thymus	75.5 ± 5.9	54.1 ± 8.2	(0.45 ± 0.02 (100 ± 4.9)	0.55 ± 0.07 (121.2 ± 16.7)	−	56.4 ± 4.6	44.3 ± 3.5	0.24 ± 0.01 (100 ± 5.6)	0.29 ± 0.03 (120.2 ± 13)	−
Heart	86.4 ± 4.3	53.9 ± 1.9	0.52 ± 0.01 (100 ± 4.1)	0.55 ± 0.03 (98.4 ± 2.7)	−	104.8 ± 4.2	64.0 ± 6.8	0.46 ± 0.01 (100 ± 1.2)	0.41 ± 0.02 (88.6 ± 4.8)	−
Lungs	247.4 ± 2.6	136.0 ± 11.7	1.50 ± 0.05 (100 ± 3.5)	1.42 ± 0.22 (94.9 ± 14.7)	−	261.3 ± 13.3	144.4 ± 20.5	1.14 ± 0.07 (100 ± 6.3)	0.91 ± 0.04 (79.5 ± 3.8)	−
Liver	838.0 ± 62.0	446.0 ± 70.2	5.04 ± 0.34 (100 ± 6.8)	4.51 ± 0.69 (89.5 ± 13.7)	−	1115.0 ± 77.7	927.5 ± 126	4.88 ± 0.4 (100 ± 8.1)	5.82 ± 0.14 (119.2 ± 2.8)	−
Spleen	58.1 ± 7.1	26.3 ± 5.4	0.35 ± 0.03 (100 ± 9.9)	0.27 ± 0.06 (76.7 ± 17.0)	−	93.4 ± 15.2	42.1 ± 7.6	0.4 ± 0.05 (100 ± 13.1)	0.26 ± 0.03 (66.1 ± 8.5)	+
Kidneys	239.9 ± 14.4	115.1 ± 11.7	1.44 ± 0.06 (100 ± 3.8)	1.16 ± 0.07 (80.7 ± 4.9)	+	285.8 ± 18.9	173.5 ± 28.1	1.24 ± 0.06 (100 ± 9.6)	1.08 ± 0.11 (87.3 ± 8.6)	+
Ovaries	4.3 ± 0.7	2.6 ± 0.6	0.03 ± 0.004 (100 ± 5.6)	0.03 ± 0.006 (87.7 ± 13)	−	9.2 ± 0.6	6.4 ± 1.2	0.04 ± 0.001 (100 ± 2.8)	0.04 ± 0.004 (99.4 ± 8.2)	−
Body (g)	20.8 ± 1.1	10.9 ± 0.6				28.6 ± 1.1	17.3 ± 1.4			
n	5	4				4	4			

[a] Relative (% of control) values ± SE shown in parentheses were derived by the same procedure described in the legend to Table 1 and then compared to evaluate statistically significant differences (Δ; see Table 1). Averages were calculated from the numbers (*n*) of animals shown.

tal growth, we intercrossed *Ghr*(+/−)/*Igf1*(+/−) double heterozygotes and also crossed to a lesser extent such heterozygotes with *Ghr*(−/−)/*Igf*(+/−) partners. We then compared progeny that we considered indiscriminately as phenotypically "normal" (i.e., wild-type or heterozygous animals for either or both of the *Ghr* and *Igf1* genes; "*W*" phenotype) with single mutants lacking either GHR ("*G*" mutant phenotype) or IGF1 ("*I*" mutant phenotype) or both (double-mutant phenotype; "*D*").

In our growth analysis, we determined body weights for a period of ~6 months, but analyzed extensively and present here the most robust portion of our dataset up to p100, a time at which the growth of mice approached closely a steady state (growth plateau). Although this phase differs between mouse strains (it occurs, for example, at ~p170 in DBA/2 mice; Goedbloed, 1975), it was attained at ~p130 in the animals that we examined, similar to ICR mice (Silbermann and Kedar, 1977).

The rate and duration of proliferation, which determines the growth process, is reflected in the progressive increase in weight until a complete balance between proliferative and apoptotic events is attained. Thus, relative growth patterns of wild-type and mutant mice can be compared from plots of weight versus developmental age (growth curves), which together with their derivatives (plots of growth rates) provide an overall informative, albeit coarse index of the growth process. It should not escape attention, however, that the conclusions from such comparisons are indicative, rather than absolute descriptions, of growth patterns because, even if experimental inaccuracies in measurements are ignored, there is considerable variability in weights within and between litters of mice at any postnatal age (in contrast to the significantly narrower weight ranges during embryogenesis). In part, this variability is due to environmental factors, including nutrition. Therefore, regression analyses become necessary, a fact emphasizing further that, conceptually, any generalizations derived from descriptions of postnatal growth have mainly a statistical character.

From a comparison of growth curves (Figs. 3a and 3b), which were derived by appropriate treatment of primary weight data (see Materials and Methods), a difference between sexes in the weights of wild-type controls (heavier males) was evident from ~p20 onward, as expected (see, for example, Goedbloed, 1974; Koops *et al.,* 1987). This gender difference is due to the emerging actions of distinct gonadal steroids resulting, for example, in sexually dimorphic patterns of pulsatility in pituitary GH secretion commencing at ~p20 (see Davey *et al.,* 1999). Interestingly, sex-dependent weight differences were not detectable in mutants lacking IGF1 or in double mutants. On the other hand, female animals lacking GHR tended to be somewhat heavier than the corresponding males, but this difference was not statistically significant. Thus, for regression analysis (Fig. 3b), the data for each mutant phenotype were lumped, regardless of sex, to increase the number of observations (Fig. 3a). This was necessary because of the wide range of recorded values, apparently due to segregation of presumptive modifiers affecting the weights of progeny from matings of animals with mixed genetic backgrounds (see Materials and Methods). Due to the nature of this analysis, minor effects of haploinsufficiency (reported to be <10% with a similar *Ghr* knockout; Coschigano *et al.,* 2000) would have been invisible and were ignored.

Independent and overlapping IGF1 and GH functions. In contrast to the neonatal dwarfism of *I* mutants (Liu *et al.,* 1993; Baker *et al.,* 1993), the birth weight of *G* mutants was normal. Prior to p10, there was no statistically significant difference in body weight between *W* mice and *G* mutants or between *I* and *D* mutants ($P > 0.05$; *t* test). After 2 postnatal weeks, however, and at later times, our comparisons showed clearly that all mutants were growth-retarded in the order $G > I > D$ (Figs. 3b and 4a).

If all of the GH actions, as reflected in whole body weight, were mediated by IGF1, the expectation was that the phenotype of the double mutants would be indistinguishable from that of *Igf1* nullizygotes. This is clearly not the case. Therefore, in terms of growth physiology, the GH and IGF1 signaling pathways serve both independent and overlapping functions. (Any IGF1-mediated GH action is defined here as a functional overlap.) To our knowledge, this is the first time that this conclusion can be reached definitively on the basis of genetic evidence.

Interestingly, when absolute growth rates were compared (Fig. 3c), it became obvious that the temporary decline in normal rate, which is always observed in wild-type mice shortly after weaning and prior to a growth spurt, coincided with the negative growth rate seen in all mutants. Moreover, the spurt in wild-type mice corresponded to mutant catch-up growth compensating for the previous weight loss. These observations suggest that the mechanism responsible for these rate shifts is probably common between *W* and mutant mice. Although this mechanism remains unknown, it is thought that it is not due to weaning per se (discussed by Boettiger and Osborn, 1938; Koops *et al.,* 1987).

When attained weight was used as a normalizing factor to transform absolute rates to specific growth rates (Fig. 3d), it was clearly seen that the latter became practically indistinguishable between genotypes (except for a minor deviation of *I* mutants) at around p40. In fact, the specific rates had declined considerably and tended toward zero (i.e., the growth of wild-type and mutant mice was approaching a steady state). Because growth at any time point is a function of growth already attained, the equalization of specific growth rates reveals that the separate and concerted actions of GH and IGF1 are postnatally important mainly between 15 and 40 days of mouse age.

Relative contributions of GH and IGF1 signaling to growth. To assess the magnitude of the independent and overlapping GH and IGF1 contributions to growth, we derived some rough estimates (Figs. 3e and 3f), according to the following considerations.

At each time point, the weight D_w of double mutants is the result of growth controlled by mechanisms unrelated to the GH/IGF1 axis (i.e., "basal weight," in regard to the GH and IGF1 actions). Therefore, if the wild-type weight is W_w, the relative contribution b of basal weight to the total body weight is $b = D_w/W_w$. In each of the single mutants, there is no overlapping GH/IGF1 function. Therefore, after subtraction of the basal weight D_w from the weight G_w of the mutant lacking GHR, but retaining IGF1, the remainder is the contribution of IGF1. Then, the relative contribution i of IGF1 to body weight is $i = (G_w - D_w)/W_w$. In an analogous calculation, the relative contribution g of GH signaling in the mutants with weight I_w (lacking IGF1, but retaining GHR function) is $g = (I_w - D_w)/W_w$. The relative contribution o of GH/IGF1 overlapping function is then $o = 1 - g - i - b$. The same quantity (o) can also be calculated from the relationships $(W_w - G_w)/W_w = g + o$ and $(W_w - I_w)/W_w = I + o$. Relative weights expressed as percentages of normal weight (%N) are derived by multiplying the calculated ratios by 100 (see Figs. 3e and 3f).
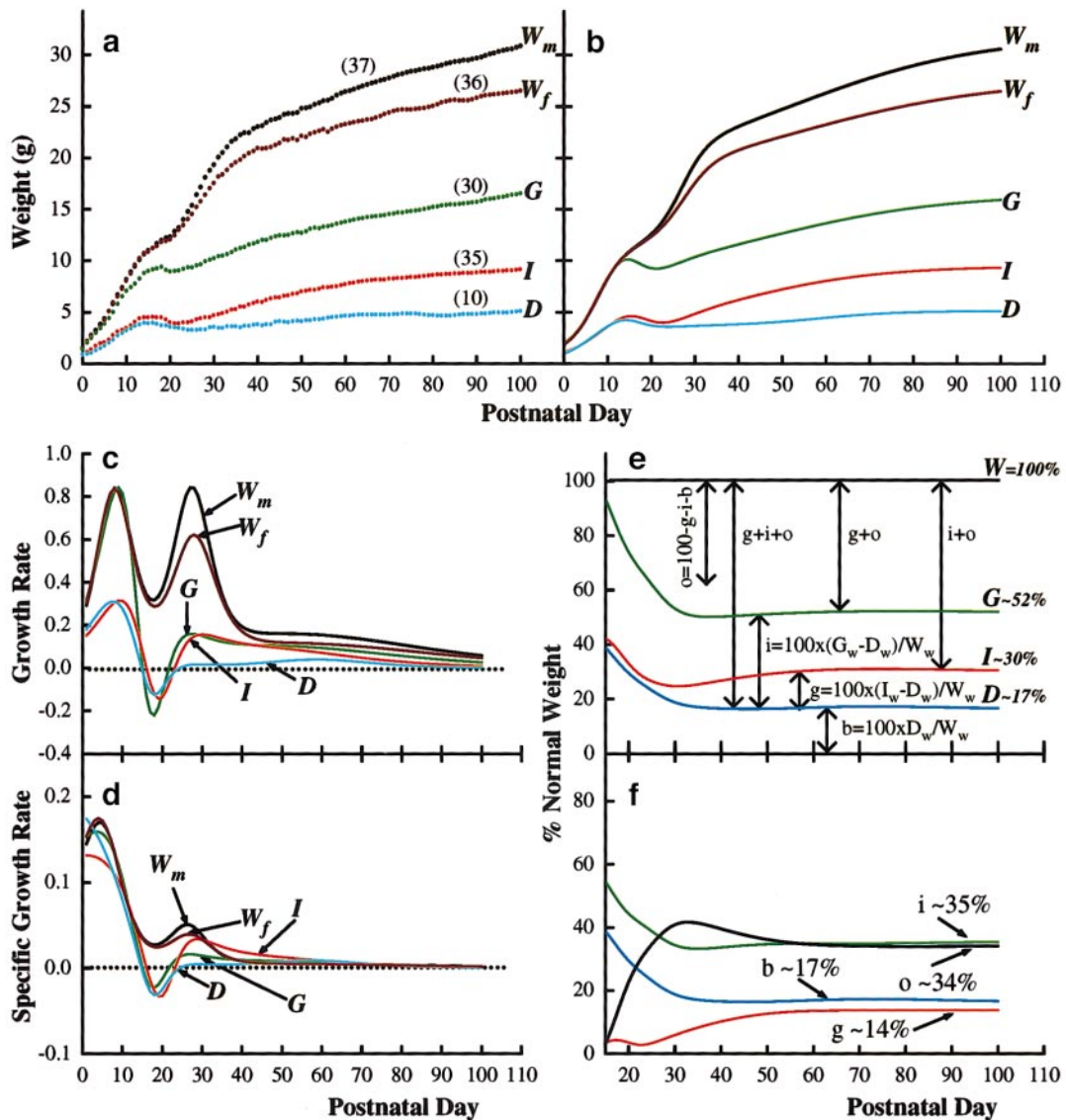
FIG. 3. Growth analysis. (a) Average growth curves of male (W_m) and female (W_f) normal animals and of mutants lacking GHR (*G*), IGF1 (*I*), or both (*D*) were derived as described under Materials and Methods (the method of analysis precludes the presentation of error flags). The number of animals of each phenotype used for determination of weights is shown in parentheses. The same growth curves are shown in (b) after regression. From the data in (b), absolute growth rates (dW/dt) and specific growth rates [(dW/dt) × ($1/W$)] were calculated and are shown in (c) and (d), respectively. Each curve point in (c) represents the difference of weights at 2 consecutive days (weight gain; g/day), whereas each point in (d) is the corresponding point in (c) divided by the average of the two weights (this ratio multiplied by 100 represents "% daily weight gain"). The data in (b) were also used to calculate relative weights (%N) for each mutant and to derive from these values estimates of the contributions to total body weight of the GH function alone (*g*), of the IGF1 function alone (*i*), and of the overlapping GH/IGF1 function (*o*), as shown in (e) and (f). The relative weight of the double mutant ("basal weight"; b) represents the contribution of growth systems unrelated to the GH/IGF1 axis. For details of the calculations, see text.

On the basis of these considerations we have estimated that at steady state ~17% of body weight has been attained by growth processes unrelated to the GH/IGF1 axis, that IGF1 makes by itself a more significant contribution than GH acting alone (35% vs 14%), and that the overlapping GH/IGF1 function makes a major contribution to total weight (34%). However, we emphasize again that these estimates are simply indicative of a growth pattern and are presented here exclusively for illustration purposes, as the exact magnitude of relative values will change by using, for
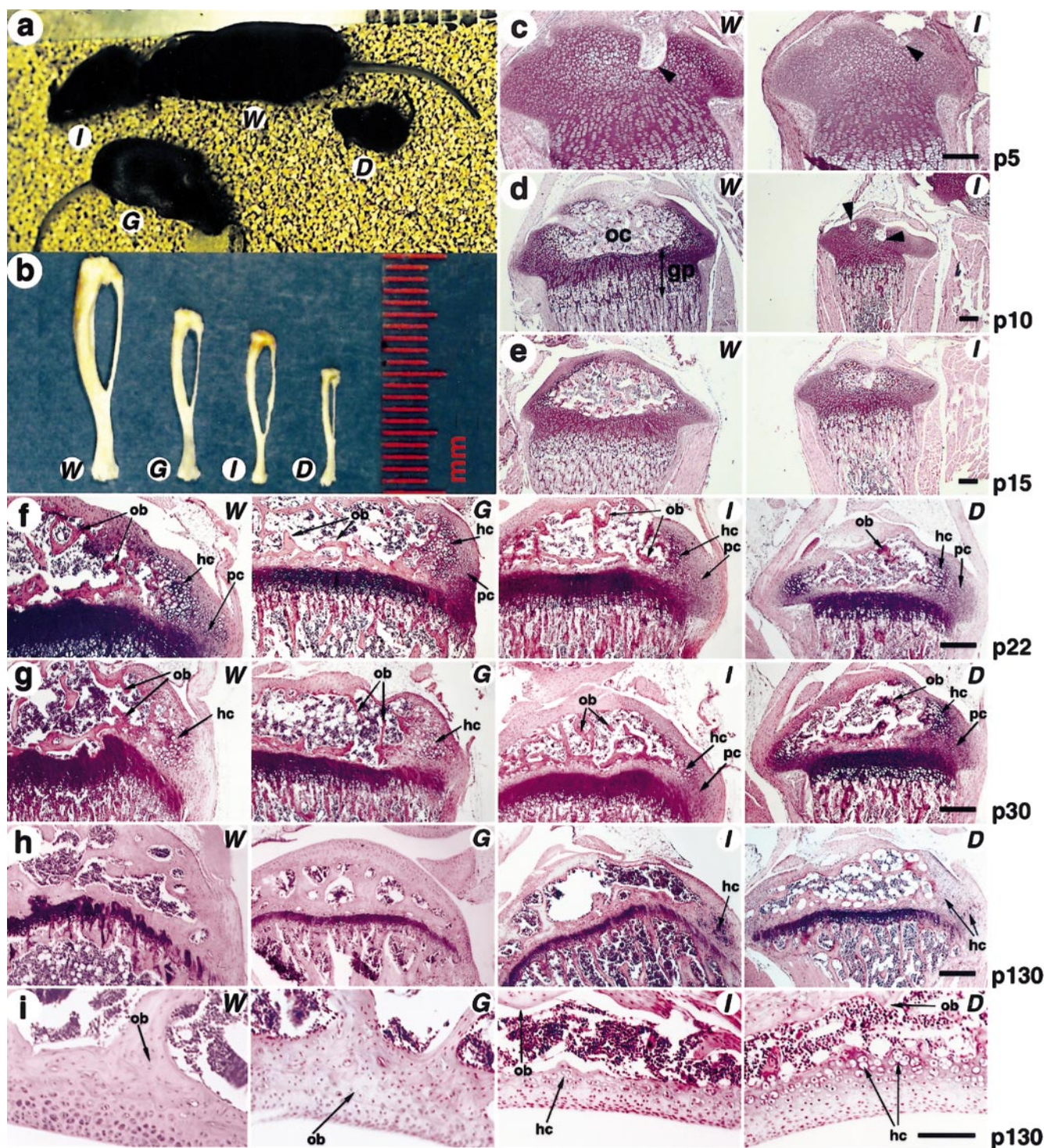
FIG. 4. (a) Example of p60 body size phenotypes of wild-type mice (*W*) and mutants lacking GHR (*G*), IGF1 (*I*), or both (*D*). (b) Tibiae from p130 mice of the same phenotypes as in (a). (c–h) Longitudinal sections of the proximal tibial epiphysis at p5 (c), p10 (d), p15 (e), p22 (f), p30 (g), and p130 (h) from mice of the indicated phenotypes. (i) Sagittal sections through the patella of the same mice as in (h). Arrowheads in (c) and (d) indicate invading vascular buds of the secondary ossification center (oc). At p10 (d), the boundaries of the growth plate (gp) are clearly defined in the wild type. Arrows in (f–h) indicate proliferative chondrocytes (pc), hypertrophic chondrocytes (hc), and ossified bone (ob). All specimens of the same age are displayed at the same magnification. The scale bar (shown once for each set of images) corresponds to 200 μm in (c–h) and to 50 μm in (i). For details, see text.

example, as wild-type weight that of female animals or by repeating the growth analyses in different genetic backgrounds. Regardless of actual levels, however, the graph with estimates of relative contributions (Fig. 3f) is still another pictorial representation of the important conclusion that after ~p40 the contribution of the GH/IGF1 system to growth is practically finished.

IGF1 and GH are key components of growth control pathways. Genes controlling growth are members of pathways serving (directly or indirectly) short- and long-range circuits of signaling interactions (autocrine/paracrine and systemic actions, respectively) that ultimately affect the performance of the cell cycle (discussed by Efstratiadis, 1998). In this regard, it can be firmly concluded from the evaluation of our genetic data (permitting the establishment of causal relationships) that, at least in rodents, the pathway in which the GH/IGF1 axis participates provides the main conduit of growth control. Additional unrelated growth control systems apparently exist, but they play relatively minor roles, since only ~17% of the total body size of an adult mouse can be attained without the participation of GH and IGF1. This value approaches the apparently lowest limit that is evolutionarily tolerable for mammalian body size, as a double *Ghr/Igf1* mutant does not exceed ~5 g in weight, which is the same as that of the smallest bat *Pipistrellus pipistrellus* and only twice the size of the smallest known mammal, the shrew *Suncus etruscus* (see Jürgens *et al.,* 1981). It should be noted that, from the point of view of IGF functions, the basal weight value of $17\%N$ is an overestimate, because the IGF2 contribution to embryonic growth has not been taken into account in the calculations presented above. Importantly, in terms of growth control, there is no opportunistic compensation by IGF2 in the absence of IGF1 and vice versa (Baker *et al.,* 1993), so that mutants lacking both of these ligands are $30\%N$ at birth. As these double *Igf1/Igf2* null mutants are not viable, it is impossible to determine the relative, steady-state body size of triple mutants also lacking GH. It can be safely hypothesized, however, that this size would have been $<17\%N$.

On the basis of our analysis, we surmise that, with the exception of a basal machinery sustaining minimal growth, all other growth control genes must be members of the circuitry involving GH/IGF1 signaling because, although they remain intact, they cannot compensate for the growth retardation of *D* mutants. The identities of such genes are progressively being revealed by knockout experiments. Some of these results confirm more or less predictable relationships between the disrupted genes and GH/IGF1 functions. For example, GH-stimulated GHR dimerizes and activates JAK2, which (among other effectors) phosphorylates STAT5b, a transcription factor activating the *Igf1* gene promoter acting either alone or synergistically with HNF1α (see Metón *et al.,* 1999; Herrington *et al.,* 2000). It was not surprising, therefore, that knockouts of the genes *Stat5b* (Udy *et al.,* 1997; Teglund *et al.,* 1998) and *Hnf1α* (Lee *et al.,* 1998) resulted in dwarfism associated with low serum IGF1.

In other cases, however, unsuspected relationships of gene functions with IGF1-mediated growth control were observed. Such examples include transgenic overexpression of IL-6 (De Benedetti *et al.,* 1997) and knockouts of the genes *Grf1* (encoding a ras guanine nucleotide exchange factor; Itier *et al.,* 1998), *Emk* (encoding ELKL motif kinase, a member of a small family of Ser/Thr protein kinases; Bessone *et al.,* 1999), and *Src3* (encoding a steroid receptor coactivator; Xu *et al.,* 2000). Moreover, it appears that even the thyroid hormone participation in growth (reviewed by Williams *et al.,* 1998) involves the GH/IGF1 axis (see Göthe *et al.,* 1999).

Is there an endocrine IGF1 function? Effective IGF1 action within an early window of developmental time provides a plausible interpretation of the results in two reports describing liver-specific, conditional knockouts of the *Igf1* gene using the *cre/loxP* system (Sjögren *et al.,* 1999; Yakar *et al.,* 1999). In both cases, the apparently unaffected average body weights of conditional mutants exhibiting significantly reduced levels of serum IGF1 were interpreted as demonstrating lack of participation of the circulating factor in growth promotion. However, ablation of endocrine IGF1 was incomplete and occurred only postnatally and relatively late, long after the aforementioned critical post-weaning period of growth spurt. It is likely that, as in analogous cases (see Postic and Magnuson, 2000), *cre*-mediated DNA excision was progressive in the population of hepatocytes, consistent with the observation that serum IGF1 was ~$50\%N$ at p26 and $23\%N$ at p42 (Yakar *et al.,* 1999) or $25.4\%N$ at p77 (Sjögren *et al.,* 1999). The presence of this residual circulating IGF1 was attributed to an unknown extrahepatic source, but this is an unlikely possibility. We think that, at least at present, the view that IGF1 participates in growth control in part by an endocrine function is still viable.

Bone Development in Mutants

Overview. To complement our study on growth based on weight analysis, we aimed to provide some information on linear growth by examining skeletal development. Specifically, we focused our study on long bones, a system in which the GH/IGF1 relationship has been studied extensively (reviewed by Ohlsson *et al.,* 1998). In this regard, we have examined in detail the proximal growth plate of the tibia, considered widely as a representative of long bone development (see, for example, Walker and Kember, 1972a,b). Consistent with this notion, we have observed that the tibial dimensions (length and width of the diaphysis and the epiphysis measured at fixed levels) retain isometric relationships to body length in both mutants and wild-type controls (Fig. 2b). We note that the relative body size relationships $W > G > I > D$ were maintained in terms of tibia dimensions (Fig. 4b and Table 3), but the differences between *G* and *I* mutants were marginal (discussed in a later section).

Because mutants lacking GHR do not differ in external

TABLE 3

Morphometric Data

	W	G	I	D
Body length (cm)				
p22	7.79 ± 0.07 (9)	6.45 ± 0.08 (6)	5.10 ± 0.07 (4)	4.10 ± 0.10 (3)
p130	10.25 ± 0.20 (8)	7.37 ± 0.10 (9)	6.77 ± 0.17 (3)	4.43 ± 0.13 (3)
Tibia length (mm)				
p22	14.33 ± 0.11 (9)	12.16 ± 0.16 (10)	9.53 ± 0.21 (4)	8.00 ± 0.26 (3)
p30	16.72 ± 0.27 (5)	13.54 ± 0.20 (5)	11.25 ± 0.05 (2)	9.3 (1)
p100	18.37 ± 0.09 (3)	13.63 ± 0.20 (3)	12.80 ± 0.26 (3)	
p130	18.28 ± 0.13 (9)	13.90 ± 0.14 (9)	12.95 ± 0.13 (6)	9.32 ± 0.14 (6)
Tibia width (mm; p130)				
Epiphysis	3.04 ± 0.07 (9)	2.30 ± 0.05 (9)	2.07 ± 0.05 (6)	1.33 ± 0.11 (6)
Diaphysis	0.96 ± 0.047 (9)	0.61 ± 0.019 (9)	0.55 ± 0.019 (6)	0.37 ± 0.021 (6)
Growth plate (proximal tibia; p22)				
Total height (μm)	314.8 ± 12.0	231.4 ± 11.7	246.2 ± 6.7	233.5 ± 12.1
"RZ" height (μm)	22.3	30.2	51.4	69.3
PZ height (μm) [A]	120.2 ± 7.4	88.9 ± 6.6	90.3 ± 8.3	70.7 ± 6.9
PZ cell number (column) [B]	17.8 ± 0.3	13.9 ± 0.6	13.4 ± 0.4	10.6 ± 0.3
PZ: 1-cell height [A/B]	6.75	6.4	6.74	6.67
HZ height (μm) [C]	172.3 ± 10.6	112.3 ± 10.8	104.5 ± 1.4	93.5 ± 4.6
HZ cell number (column) [D]	7.8 ± 0.2	6.9 ± 0.3	6.7 ± 0.1	6.5 ± 0.1
HZ: 1-cell height [C/D]	22.1	16.28	15.6	14.38
HZ cell number in 0.024 mm^2	48.2 ± 1.6	71.5 ± 1.9	75.4 ± 1.2	77.0 ± 3.4
HZ: 1-cell area (μm^2)	496.3 ± 16.7	334.0 ± 9.1	316.3 ± 5.0	311.6 ± 14.7
HZ last cell (μm)	32.7 ± 0.3	25.8 ± 0.2	26.6 ± 0.6	24.7 ± 0.3
BrdU (%; PZ)	18.7 ± 0.6	11.8 ± 0.9	11.7 ± 0.8	8.02 ± 0.2
Growth plate (proximal tibia; p30)				
Total height (μm)	242.3 ± 20.7	184.0 ± 9.7	184.5 ± 7.7	171.4 ± 4.7
"RZ" height (μm)	6.9	25.5	37.1	51.8
PZ height (μm)	106.7 ± 7.4	72.9 ± 4.8	73.0 ± 1.8	57.3 ± 1.5
PZ cell number	17.9 ± 0.9	12.9 ± 0.2	13.9 ± 0.2	10.2 ± 0.4
HZ height (μm)	128.7 ± 9.6	85.6 ± 4.5	74.4 ± 0.8	62.3 ± 3.9
HZ cell number	6.3 ± 0.2	5.4 ± 0.1	5.4 ± 0.2	5.3 ± 0.2

Note. The length and width dimensions represent mean ± SE values (averaged from the numbers of animals shown in parentheses). The total height of each growth plate represents the distance between two chondrosseous junctions. The heights of the "resting" ("RZ"), proliferative (PZ), and hypertrophic (HZ) zones were measured as described under Materials and Methods. To derive average values for each growth plate parameter measured, 4 animals were analyzed for each phenotype at p22, whereas at p30, the number was 3 (wild-type mice and *Ghr* and *Igf1* null mutants) or 2 (double mutants). Seven measurements were taken per section, using three sections per animal (21 measurements per animal). To provide an estimate for the average size of a hypertrophic chondrocyte for each phenotype, cell numbers were counted in a fixed area of 23,831 μm^2.

phenotype from wild-type mice until p15, we compared only *W* and *I* mice at early postnatal ages (p5–p15; Figs. 4c–4e) and began comparing all four phenotypes at p22 and other more advanced ages (Figs. 4f–4i). From these analyses, we conclude that the *Igf1* and *Ghr* mutations or their combination does not result in histologically dysmorphic or disorganized skeletogenic tissues (absence of histopathological changes). In fact, all of our morphological observations can be interpreted as indicative of developmental delays due to hypoproliferation, in combination with a reduced size of hypertrophic chondrocytes. Below, we present the evidence supporting these conclusions.

Delayed development of secondary ossification centers. Long bones grow in length by endochondral ossification (a template of cartilage formed from mesenchyme is replaced by bone; Cancedda *et al.,* 1995). Increase in length occurs by bone formation on the diaphyseal side of the growth plate (Hunziker, 1994). Chondrocytes in this cartilaginous disc (located between each semispherical epiphysis and the cylindrical diaphysis) proliferate, forming characteristic columns with spatial polarity toward the diaphyseal side (Abad *et al.,* 1999), and then differentiate, becoming hypertrophic and laying down calcifying cartilaginous matrix, before undergoing apoptosis (Gibson, 1998; Horton *et al.,*
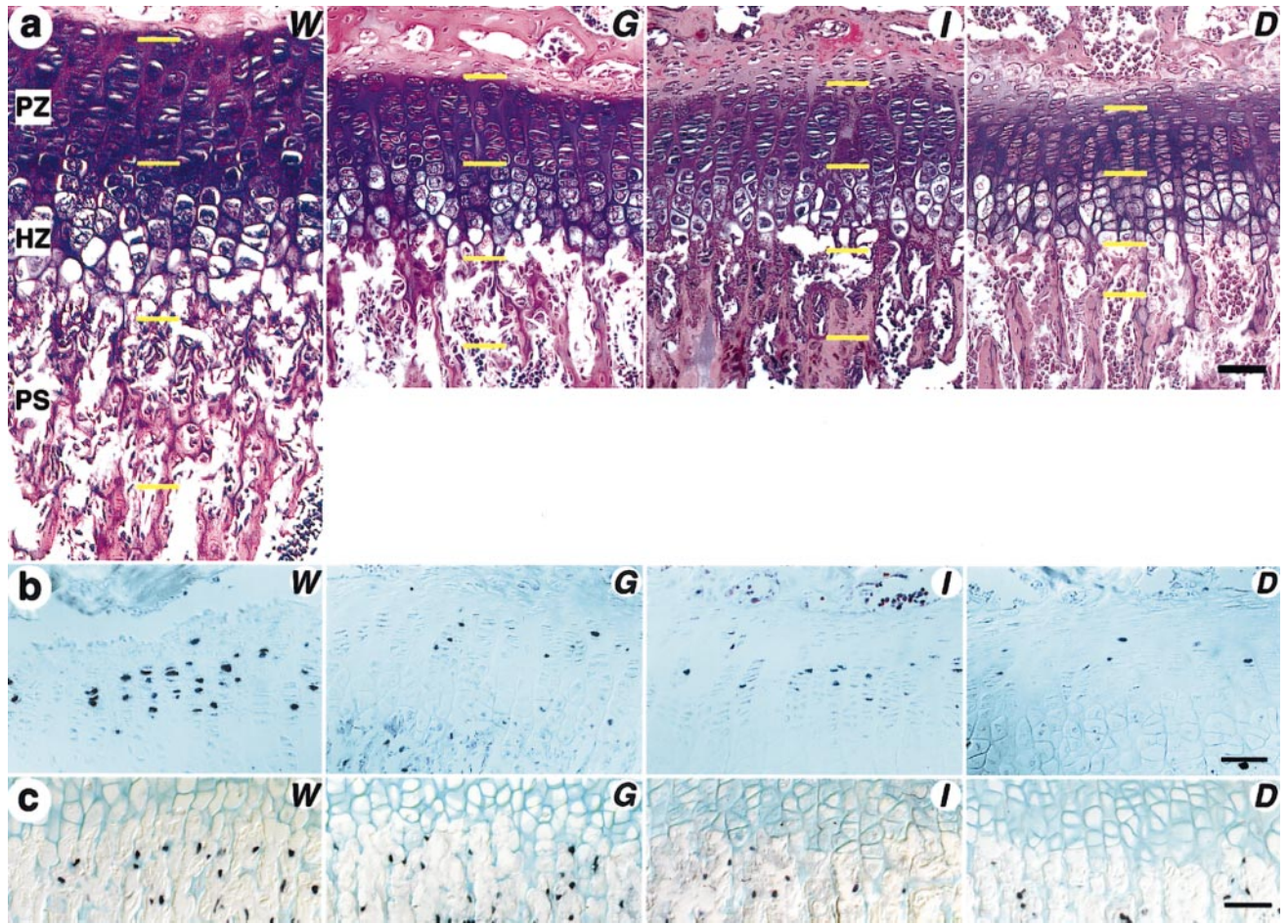
FIG. 5. (a) Histological comparison at high magnification of growth plates and their adjacent regions between the indicated wild-type and mutant phenotypes at p30 (see Fig. 3g), to display in detail the reduction in the mutant specimens of the height of chondrocyte zones (PZ, proliferative zone; HZ, hypertrophic zone; see also Table 3) and of the primary spongiosa (PS). The approximate borders between zones are indicated with yellow horizontal bars (considering the upper limit of the darkly staining round cells of the bone marrow as the bottom of the primary spongiosa). (b) BrdU labeling of chondrocytes in the growth plates of the proximal tibia (specimens from mice with the indicated phenotypes at p22). The staining appears as dark blue. There are clearly fewer labeled chondrocytes in the mutants (see text and Table 3). (c) BrdU labeling of stromal cells in the primary spongiosa [specimens as in (b)] indicating that there is also hypoproliferation of osteoblasts in the mutants. All scale bars correspond to 50 μm.

1998). Vessels invading the cartilage bring with them perivascular mesenchymal cells, some of which are osteoblasts that deposit bone matrix on the calcified cartilaginous template forming metaphyseal trabecular bone (primary spongiosa). The capillaries and osteoblasts that are the first to invade constitute an ossification center. This process continues until epiphyseal closure (fusion between the epiphysis and the diaphysis), although, in contrast to humans, this state is approached, but apparently not completed in particular rodent growth plates, including that of the proximal tibia (see Dawson, 1935; Walker and Kember, 1972b).

The same ossification steps take place in the epiphysis itself, but in this case the chondrocytes, which are solitary or present in small clusters rather than being arranged in columns, differentiate from flat proliferating cells at the periphery of the cartilage to enlarged hypertrophic cells toward the center. Thus, ossification in this region spreads from a secondary ossification center radially, whereas the earlier ossification in the diaphysis spreads from a primary center proximally and distally in a cylinder forming a bone marrow cavity.

The first appearance of secondary ossification centers in a particular bone occurs always postnatally, but the time varies widely between mouse strains (see, for example, Johnson, 1933; Wirtschafter, 1960; Floyd *et al.,* 1987; Patton and Kaufman, 1995). Initially, the population of cells in the cartilaginous epiphysis is morphologically quite homoge-
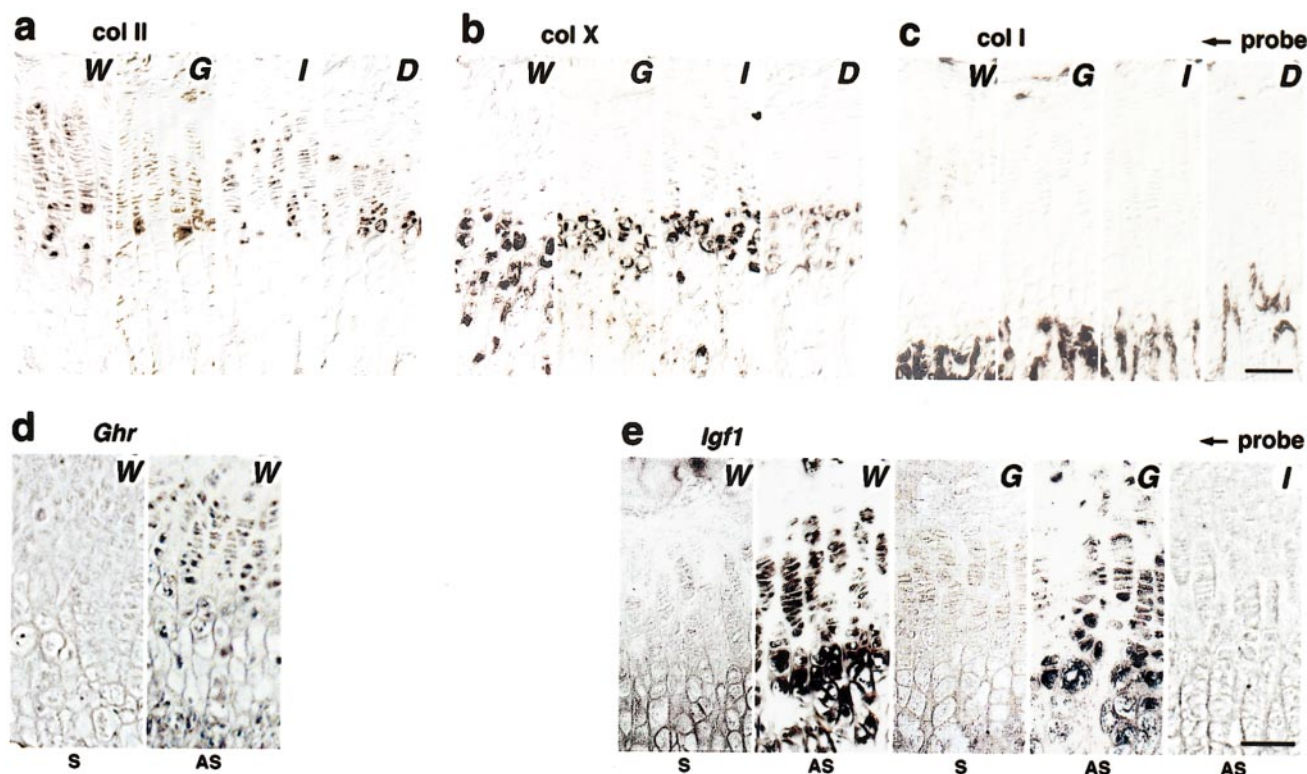
FIG. 6. *In situ* hybridization analysis of gene expression in proximal tibia sections at p22. The probes used are indicated at the top. (a–c) In all four phenotypes, transcripts for the examined collagen types (II, X, and I) are expressed in appropriate types of cells, although there may be some variability in signal intensity (dark staining). The thickness of the layers expressing these markers correlates with the measurements in Table 3. (d) In wild-type mice (*W*), hybridization signal signifying *Ghr* expression is detected unequivocally in proliferative chondrocytes with an antisense (AS) but not with a (control) sense (S) probe. *Ghr* null mice were not used as negative controls because they continue to express a modified transcript (Figs. 1c and 1d). (e) *Igf1* gene expression was detected with an antisense probe in proliferative and hypertrophic chondrocytes in both wild-type and *Ghr* null mice. The negative controls (*Igf1* sense probe for wild-type and *Ghr* null mice and *Igf1* antisense probe for *Igf1* null mice) did not show staining. All scale bars correspond to 50 µm.

neous and a demarcation between epiphyseal and growth plate chondrocytes is not discernible. However, lineage specification has probably already occurred, according to a model postulating two distinct endochondral ossification processes (Vu *et al.,* 1998): one occurring in growth plate chondrocytes, expressing for example *Ihh* (Iwasaki *et al.,* 1997), and a different one in epiphyseal chondrocytes that remain *Ihh*-negative.

At the earliest time point that we have examined (p5), we observed that, in both wild-type controls and *Igf1* nullizygotes, columns of chondrocytes present in the presumptive region of the developing growth plate could already be discriminated from epiphyseal chondrocytes. Still, the epiphysis was entirely cartilaginous and characterized by invading vascular buds signifying the initiation of formation of a secondary ossification center (Fig. 4c, arrowheads). The bud in the *Igf1* mutant, however, was barely detectable in comparison with that in the wild-type control that had reached a more advanced stage.

Five days later (p10), the formation of the secondary

ossification center had progressed significantly in the control, whereas in a corresponding *Igf1* null specimen, despite some advancement, only two small ossifying regions were discernible (Fig. 4d, arrowheads). At p15 (Fig. 4e), notwithstanding further progress of the ossification process in the *Igf1* mutant, the delay in the formation of the secondary ossification center exceeded 5 days, as the development of this structure had not yet reached the stage that the control specimen had attained at p10. Additional comments about the development of secondary ossification centers in all of the mutants are made below in the context of a comparison of epiphyseal bone formation.

Histological analyses of growth plates. Classically, three zones of chondrocytes (occasionally with further subdivisions) are described in the growth plate: resting (germinal or reserve), proliferative, and hypertrophic. The rather flat chondrocytes in the proliferative zone divide actively and their spatial organization in columns represents the temporal progression of an ordered differentiation process, as they pass through well-defined stages character-

ized by changes in shape and size and deposition of extracellular matrix components. More distally, toward the diaphyseal border of the growth plate, cells become more spherical and increase in size prior to their death at the cartilage/bone junction. Although this process is universally referred to as "hypertrophy," it does not appear to be a true increase in cellular constituents, but is rather a swelling due to an increase in water content by an unknown mechanism, potentially accompanied by cytoskeletal rearrangements (see Farquharson *et al.,* 1999).

In contrast to proliferative and hypertrophic cells, we think that the identity and role of resting chondrocytes remain an open issue (see also Price *et al.,* 1994; Nuttall *et al.,* 1999; Bailón-Plaza *et al.,* 1999). This cell population has been described quite often as including at least a subset of presumptive stem cells (see Kember, 1971, 1978; Buckwalter *et al.,* 1985; Hunziker, 1994), but to our knowledge no criteria or markers allowing their identification were ever assigned and, despite some attempts (see, for example, Ohlsson *et al.,* 1992), no hard evidence was ever presented to demonstrate that resting cells are the immediate precursors of proliferative chondrocytes. In fact, the resting zone is defined only morphologically as a population of mostly solitary cells occupying the space between the bone being formed in the secondary ossification center and the zone of proliferative chondrocytes (columns). Accordingly, as the secondary ossification center expands, the resting zone is continuously shrinking, so that it is impossible to make a distinction between resting chondrocytes and the epiphyseal cartilaginous elements at the moving front of the forming bone toward the growth plate. Thus, if a developmental delay occurs, as is the case with *G*, *I*, and *D* mutants, the resting zone, recognized exclusively on the basis of histological position, will appear as enlarged. This could be quite misleading. For example, a comparison of growth plates between normal and *Igf1* null mice (Wang *et al.,* 1999) led, in our opinion, to the unfounded interpretation that there is an expansion of the resting zone in the mutants as a consequence of enhanced GH activity due to the absence of IGF1 and elimination of the negative feedback in GH secretion. At present, we prefer to maintain an agnostic position and have avoided interpretations in regard to the resting zone, which we have defined as the remainder after subtracting from the height of the growth plate (distance between the two chondrosseous junctions) the sum of the heights of the proliferative and hypertrophic zones (Table 3).

Comparison of histological sections of the proximal tibia regions between *W*, *G*, *I*, and *D* mice at p22 and p30 revealed that both the proliferative and the hypertrophic zones of chondrocytes were shorter in the mutants in the same order as for lengths and weights ($W > G > I > D$; Table 3 and Fig. 5a). The average height of the proliferative zone in each of the phenotypes was found to be proportional to cell number. Therefore, proliferative cell size was normal in all three mutants (Table 3; compare A/B ratios at p22; average cell height of 6.64 ± 0.08 μm). In contrast, the average height of a hypertrophic chondrocyte in the mutants (same for all; 15.4 ± 0.55 μm; see C/D ratios, Table 3), was only ~70% of the corresponding dimension in the controls (22.1 μm). A similar ratio (~65%) was calculated from the results of counting hypertrophic cell numbers in a fixed area of known dimensions (Table 3). Although the mechanism resulting in this alteration is unknown, this is the only observation that can be interpreted as suggesting that the GH/IGF system may be involved not only in proliferative events but also in differentiation of chondrocytes toward a hypertrophic state.

Overall, our observations allow the following interpretation concerning the reduction of bone length in the mutants. The rate of longitudinal bone growth is considered to be a function of the rate of proliferation in the columns and of the height of the terminal hypertrophic chondrocytes (Kember, 1993). In fact, there is an apparent positive linear relationship between the rate of longitudinal bone growth and the volume of hypertrophic chondrocytes (Breur *et al.,* 1991). We think that hypoproliferation in the zone of actively dividing chondrocytes results in a reduction in the rate of production and maturation of hypertrophic zone chondrocytes in our mutants, leading in turn to a significant reduction in the height of the primary spongiosa (Fig. 5a). As a consequence, the mutants have shorter bones. The same relationships, including reduced heights of the primary spongiosa, were also observed in distal femora examined at p60 (data not shown).

Parallel ossification delays were observed in epiphyseal chondrocytes, but predominantly in *I* and *D* mutants. In contrast, the secondary ossification center of the *G* mutants did not differ dramatically from wild-type at the examined ages (p22 and p30), possibly because the ossification process had progressed significantly by the time the effects of the *Ghr* mutation were first manifested (p15). At p30, most of the epiphyseal chondrocytes in *W* and *G* mice were already hypertrophic, whereas abundant proliferating chondrocytes were still detectable in the epiphyses of *I* and *D* mutants (Fig. 4g). This difference in the pace of the differentiation program was further evident at p130 (Fig. 4h). Thus, the *W* and *G* mice had practically reached a steady state, and their growth plates were approaching closure, while the epiphyses were completely converted into bone. In contrast, hypertrophic chondrocytes were still discernible in the epiphyses of *I* and *D* mutants. Analogous observations were made in the patella (a bone also developing by endochondral ossification), which at p130 illustrates very characteristically the relative ossification delays in the mutants (Fig. 4i).

Proliferation assays. To examine whether our interpretation (postulating hypoproliferation as the cause of our morphological observations) could be supported by direct evidence, we assessed the effects of the *Ghr* and *Igf1* mutations on chondrocyte proliferation by BrdU labeling for 1 h prior to sacrifice. Considering that the duration of the S phase in mouse chondrocytes is ~7 h (~36 h average cell cycle time; Vanky *et al.,* 1998), the brief pulse of BrdU could identify exclusively S-phase proliferating cells, thus

providing an index of proliferative activity. The fraction of proliferative zone chondrocytes that incorporated BrdU in wild-type mice was 18.7%. Considering this value as normal (100% of attainable incorporation), we observed a significant reduction in all of the mutants (the corresponding value was ~63%N in G or I mutants and ~43%N in D mutants; Table 3). In agreement with previous evidence (Vanky *et al.,* 1998), incorporation was observed only in the upper 60% of the proliferative zone (Fig. 5b). This snapshot of BrdU labeling indices is consistent with our interpretation of reduced chondrocyte proliferation as a consequence of the mutations under study. Diminished incorporation was also observed in the stromal cells of the mutants (Fig. 5c). Although detailed counting of these cells representing the presumptive precursors of osteoblasts was not performed, we noticed that their numbers were reduced in the mutants. We note that, in a previous study (Wang *et al.,* 1999), a difference in BrdU labeling indices in proliferative zone chondrocytes was not observed between wild-type and *Igf1* null mice, for unknown reasons.

In situ hybridization analyses. From our comparative histological analysis we concluded that, except for the size of hypertrophic chondrocytes, differentiation defects or histopathological changes were absent from our mutants. To support this conclusion further, we performed *in situ* hybridization analysis to examine the expression of collagen markers. In particular, we tested for expression of type II collagen mRNA occurring predominantly in proliferating chondrocytes, for expression of type X collagen mRNA that is restricted to hypertrophic chondrocytes, and for expression of type I collagen mRNA that is restricted to osteoblastic cells (see Lee *et al.,* 1994). Comparative analysis of the results (Figs. 6a–6c) did not reveal any differences in signal localization between mutants and controls, although subtle, and difficult to assess, differences in signal intensity may exist.

Importantly, we also used *in situ* hybridization analysis to examine the expression of *Ghr* and *Igf1* in the growth plate. Such information was crucial for interpretation of the GH and IGF1 relationship in bone development, especially considering that previously reported data are either incomplete or conflicting.

To our knowledge, *Ghr* expression in the proximal tibial epiphysis has not been examined by *in situ* hybridization, but data from immunohistochemical analyses of rat specimens are available. In two of three studies (Symons *et al.,* 1996; Vidal *et al.,* 1997), all using the same monoclonal antibody, stained cells were localized in the articular and epiphyseal cartilage, the secondary ossification center, the resting zone of chondrocytes, and also in the primary spongiosa and bone marrow cells. However, the proliferative and hypertrophic chondrocytes were reportedly negative for immunostaining. In contrast, in a third study (Edmondson *et al.,* 2000), a positive signal was detected immunohistochemically in proliferative chondrocytes, in agreement with similar results for rabbit and human growth plates (Barnard *et al.,* 1988; Werther *et al.,* 1990).

In rodents, immunoreactivity for IGF1, and also for type 1 IGF receptor (IGF1R), was detected in cells of the articular and epiphyseal cartilage, secondary ossification centers, proliferating (but not hypertrophic) chondrocytes, and bone marrow cells (Joseph *et al.,* 1999; Maor and Karnieli, 1999; Kikkawa *et al.,* 2000). On the other hand, *Igf1* expression examined in rats and mice by *in situ* hybridization at various postnatal ages up to 7 weeks (Shinar *et al.,* 1993; Wang *et al.,* 1995) indicated the presence of transcripts in perichondrium, periosteum, and presumptive osteoblasts of epiphyseal and metaphyseal trabecular bone, but not in growth plate chondrocytes, which nevertheless appeared to express *Igf1r* (Wang *et al.,* 1995). These results, however, were not in agreement with other *in situ* hybridization reports (Nilsson *et al.,* 1990; Lazowski *et al.,* 1994; Hanna *et al.,* 1995) showing *Igf1* expression in rat growth plate chondrocytes. It is likely that, because of low levels of *Igf1* transcription in chondrocytes, detection of signal by *in situ* hybridization, which is feasible under conditions of induced expression (see, for example, Rihani-Bisharat *et al.,* 1998), may depend on assay sensitivity.

The uncertainty about the expression of *Ghr* and *Igf1* genes in the same cells, and more specifically in proliferating chondrocytes, generated vexing questions in regard to the interpretation of our morphological and BrdU incorporation results. Therefore, we attempted to evaluate the situation directly by performing nonradioactive *in situ* hybridization experiments of high sensitivity (see Materials and Methods). In tibia sections from wild-type mice, we observed reproducibly a relatively weak, but specific, hybridization signal for *Ghr* transcripts in proliferating chondrocytes using an antisense probe, whereas the results with a sense (control) probe were negative (Fig. 6d). Similarly, positive hybridization signal for *Igf1* was detected in the same cells (and in addition in hypertrophic chondrocytes) with an antisense, but not with a sense, probe (Fig. 6e). In fact, the results with a sense probe were indistinguishable from those obtained with an antisense probe using sections from *Igf1* null mutants. Importantly, when these experiments were repeated with mutants lacking GHR, the results showed unequivocally that *Igf1* gene expression was retained in the absence of GH action (Fig. 6e). It was not possible, however, to ascertain whether the level of expression was normal or reduced.

The dual effector theory is not tenable. Our analysis of linear growth, although not extensive, revealed that GH and IGF1 have independent and overlapping functions in chondrocytes, since the phenotype of double mutants is more severe than that manifested in either class of single mutant. However, in contrast with the important interdependence between the GH and the IGF1 signaling roles in terms of whole body weight, the independent actions of these growth effectors appear to predominate in chondrocytes, whereas their overlapping function has secondary significance. Thus, when the values for body or tibia length at steady state (p130; Table 3) are taken into consideration, the sum of the deficits of the G and I single mutants from

wild type is only slightly larger than the corresponding deficit of the double mutant, revealing that the contribution of overlapping function to bone growth does not exceed ~5% of the total (details of the calculations are not shown). Whether this functional overlap of small magnitude consists of two components, GH-induced IGF1 function in chondrocytes and endocrine function of IGF1, cannot be ascertained from our results.

Consistent with our conclusion that in chondrocytes the independent GH and IGF1 actions predominate, we found that the degree of hypoproliferation, as assessed by histological and BrdU incorporation data, did not differ in magnitude between mutants lacking IGF1 or GHR, and yet the same cell population (proliferating chondrocytes) was affected. These observations do not support the dual effector theory, which was initially proposed for adipocytes (Green *et al.,* 1985) and later adapted for chondrocytes (Green *et al.,* 1985; Isaksson *et al.,* 1987). This theory posits that GH action is essential for promotion of the differentiation of progenitor cells (resting zone prechondrocytes), whereas IGF1 acts on proliferating chondrocytes as a mitogen and stimulates subsequent clonal expansion. Thus, a postulate that was repeatedly emphasized (see Ohlsson *et al.,* 1998, and other references therein) is that GH and IGF1 act on different growth plate cell populations (or compartments). This view is clearly inconsistent with our results demonstrating that both *Igf1* and *Ghr* are expressed in the same zone of proliferative chondrocytes, that they are functionally equally potent and almost completely independent, that they are both involved in proliferation, and that differentiation resulting in the appearance of chondrocyte columns does occur in the absence of either or both of these effectors.

CONCLUDING REMARKS

Taking into consideration the genetic evidence that we have provided, the components of the GH/IGF1 relationship can be viewed as follows. GH is involved in the production of hepatic IGF1, which reaches the circulation and behaves as a *bona fide* hormone (the classic "somatomedin"). It is notable, in this regard, that injections of this factor are known to augment growth reproducibly (see, for example, van Buul-Offers *et al.,* 1986, 1988, 2000; Chatelain *et al.,* 1991; Hunziker *et al.,* 1994). This endocrine function (component 1) corresponds to the overlapping activity of GH and IGF1, together with some relatively minor overlap of GH-dependent IGF1 production in a few extrahepatic tissues (component 2). In the majority of extrahepatic tissues, however, GH and IGF1 act independently (components 3 and 4). Whole body growth is mostly manifested as the sum of variable effects of these components in various tissues.

When GH is lacking, as is the case in Snell and *lit* mutants, administration of GH has greater effect than administration of IGF1 because, in the GH/IGF1 relationship, GH is upstream and also has independent action. Although the circulating IGF1 is diminished in the absence of GH, the local (GH-independent IGF1) is still active. Thus, administration of IGF1 simply restores the missing endocrine function. This function is also restored by GH administration and, in addition, the missing IGF1-independent GH actions are also restored (greater sum of activity). Similarly, because of the described relationships, wild-type animals respond more to GH than to IGF1 administration (normal functions are augmented; Won and Powell-Braxton, 1998). In contrast to normal mice or mutants lacking GH, the growth of mutants lacking IGF1 improves only by IGF1 administration (Won and Powell-Braxton, 1998). These mice appear to remain unresponsive to GH (Won and Powell-Braxton, 1998; Liu and LeRoith, 1999) because GH alone makes a relatively small contribution to growth, as we have shown here, which is potentially counterbalanced by inhibition of GHR dimerization due to ligand excess (see Daughaday, 1997). In fact, excess is extreme in this case, since exogenous GH is added to the already increased concentration of circulating hormone due to the absence of the negative feedback loop.

It is notable that, although under normal circumstances, there is very significant GH/IGF1 functional overlap in terms of whole body growth, in artificial cases of overexpression, compensatory effects of large magnitude are possible exactly because of the independence of the GH and IGF1 components, as revealed by the following classic experiment. IGF1 overexpression in transgenic mice resulted in a 30% increase of body weight over normal that was accompanied by a 50% increase in serum IGF1 (Mathews *et al.,* 1988). When these transgenics were crossed with dwarf transgenic mice lacking GH (pituitary somatotrophs were ablated by diphtheria toxin expression; Behringer *et al.,* 1988), the progeny were indistinguishable from wild type, despite the absence of GH (Behringer *et al.,* 1990). Also, quite remarkably, high GH expression in the liver from an adenovirus construct was able to reverse completely the phenotype in *lit* mice by catch-up growth (Hahn *et al.,* 1996).

Our results, placed in the framework of the growth control field, indicate that the IGF system is the major determinant of both embryonic and postnatal growth that is modulated in the postnatal period by GH. Thus, the GH and IGF1 effectors, acting in concert, participate in the convergence of most growth signaling pathways. Although details about their exact relationship are still missing, we think that the simple view of a four-component system presented above is not only compatible with most of the available evidence, but can also serve as a springboard for further experimental testing.

ACKNOWLEDGMENTS

REFERENCES

Abad, V., Uyeda, J. A., Temple, H. T., De Luca, F., and Baron, J. (1999). Determinants of spatial polarity in the growth plate. *Endocrinology* **140,** 958–962.

Bailon-Plaza, A., Lee, A. O., Veson, E. C., Farnum, C. E., and van der Meulen, M. C. (1999). BMP-5 deficiency alters chondrocytic activity in the mouse proximal tibial growth plate. *Bone* **24,** 211–216.

Baker, J., Liu, J. P., Robertson, E. J., and Efstratiadis, A. (1993). Role of insulin-like growth factors in embryonic and postnatal growth. *Cell* **75,** 73–82.

Baker, J., Hardy, M. P., Zhou, J., Bondy, C., Lupu, F., Bellve, A. R., and Efstratiadis, A. (1996). Effects of an *Igf1* gene null mutation on mouse reproduction. *Mol. Endocrinol.* **10,** 903–918.

Barnard, R., Haynes, K. M., Werther, G. A., and Waters, M. J. (1988). The ontogeny of growth hormone receptors in the rabbit tibia. *Endocrinology* **122,** 2562–2569.

Behringer, R. R., Mathews, L. S., Palmiter, R. D., and Brinster, R. L. (1988). Dwarf mice produced by genetic ablation of growth hormone-expressing cells. *Genes Dev.* **2,** 453–461.

Behringer, R. R., Lewin, T. M., Quaife, C. J., Palmiter, R. D., Brinster, R. L., and D'Ercole, A. J. (1990). Expression of insulin-like growth factor I stimulates normal somatic growth in growth hormone-deficient transgenic mice. *Endocrinology* **127,** 1033–1040.

Berelowitz, M., Szabo, M., Frohman, L. A., Firestone, S., and Hintz, R. L. (1981). Somatomedin-C mediates growth hormone negative feedback by effects on both the hypothalamus and the pituitary. *Science* **212,** 1279–1281.

Bessone, S., Vidal, F., Le Bouc, Y., Epelbaum, J., Bluet-Pajot, M. T., and Darmon, M. (1999). EMK protein kinase-null mice: Dwarfism and hypofertility associated with alterations in the somatotrope and prolactin pathways. *Dev. Biol.* **214,** 87–101.

Bishop, K. M., and Wahlsten, D. (1999). Sex and species differences in mouse and rat forebrain commissures depend on the method of adjusting for brain size. *Brain Res.* **815,** 358–366.

Boettiger, E., and Osborn, C. M. (1938). A study of natural growth and ossification in hereditary dwarf mice. *Endocrinology* **22,** 447–457.

Breier, B. H., Gallaher, B. W., and Gluckman, P. D. (1991). Radioimmunoassay for insulin-like growth factor-I: Solutions to some potential problems and pitfalls. *J. Endocrinol.* **128,** 347–357.

Breur, G. J., VanEnkevort, B. A., Farnum, C. E., and Wilsman, N. J. (1991). Linear relationship between the volume of hypertrophic chondrocytes and the rate of longitudinal bone growth in growth plates. *J. Orthop. Res.* **9,** 348–359.

Buckwalter, J. A., Mower, D., Schafer, J., Ungar, R., Ginsberg, B., and Moore, K. (1985). Growth-plate-chondrocyte profiles and their orientation. *J. Bone Joint Surg. Am.* **67,** 942–955.

Butler, A. A., Ambler, G. R., Breier, B. H., LeRoith, D., Roberts, C. T., and Gluckman, P. D. (1994). Growth hormone (GH) and insulin-like growth factor-I (IGF-I) treatment of the GH-deficient dwarf rat: Differential effects on IGF-I transcription start site expression in hepatic and extrahepatic tissues and lack of effect on type I IGF receptor mRNA expression. *Mol. Cell. Endocrinol.* **101,** 321–330.

Cancedda, R., Descalzi Cancedda, F., and Castagnola, P. (1995). Chondrocyte differentiation. *Int. Rev. Cytol.* **159,** 265–358.

Chandrashekar, V., Bartke, A., Coschigano, K. T., and Kopchick, J. J. (1999). Pituitary and testicular function in growth hormone receptor gene knockout mice. *Endocrinology* **140,** 1082–1088.

Chatelain, P. G., Sanchez, P., and Saez, J. M. (1991). Growth hormone and insulin-like growth factor I treatment increase testicular luteinizing hormone receptors and steroidogenic responsiveness of growth hormone deficient dwarf mice. *Endocrinology* **128,** 1857–1862.

Cheng, T. C., Beamer, W. G., Phillips, J. A., Bartke, A., Mallonee, R. L., and Dowling, C. (1983). Etiology of growth hormone deficiency in little, Ames, and Snell dwarf mice. *Endocrinology* **113,** 1669–1678.

Coschigano, K. T., Clemmons, D., Bellush, L. L., and Kopchick, J. J. (2000). Assessment of growth parameters and life span of GHR/BP gene-disrupted mice. *Endocrinology* **141,** 2608–2613.

Dawson, A. B. (1935). The influence of hereditary dwarfism on the differentiation of the skeleton of the mouse. *Anat. Rec.* **61,** 485–493.

Daughaday, W. H. (1989). A personal history of the origin of the somatomedin hypothesis and recent challenges to its validity. *Perspect. Biol. Med.* **32,** 194–211.

Daughaday, W. H. (1997). Sulfation factor revisited: The one–two punch of insulin-like growth factor-I action on cartilage. *J. Lab. Clin. Med.* **129,** 398–399.

Davey, H. W., Wilkins, R. J., and Waxman, D. J. (1999). STAT5 signaling in sexually dimorphic gene expression and growth patterns. *Am. J. Hum. Genet.* **65,** 959–965.

De Benedetti, F., Alonzi, T., Moretta, A., Lazzaro, D., Costa, P., Poli, V., Martini, A., Ciliberto, G., and Fattori E. (1997). Interleukin 6 causes growth impairment in transgenic mice through a decrease in insulin-like growth factor-I. A model for stunted growth in children with chronic inflammation. *J. Clin. Invest.* **99,** 643–650.

DeChiara, T. M., Efstratiadis, A., and Robertson, E. J. (1990). A growth-deficiency phenotype in heterozygous mice carrying an insulin-like growth factor II gene disrupted by targeting. *Nature* **345,** 78–80.

DeChiara, T. M., Robertson, E. J., and Efstratiadis, A. (1991). Parental imprinting of the mouse insulin-like growth factor II gene. *Cell* **64,** 849–859.

Edens, A., Southard, J. N., and Talamantes, F. (1994). Mouse growth hormone-binding protein and growth hormone receptor transcripts are produced from a single gene by alternative splicing. *Endocrinology* **135,** 2802–2805.

Edmondson, S. R., Baker, N. L., Oh, J., Kovacs, G., Werther, G. A., and Mehls, O. (2000). Growth hormone receptor abundance in tibial growth plates of uremic rats: GH/IGF-I treatment. *Kidney Int.* **58,** 62–70.

Efstratiadis, A. (1998). Genetics of mouse growth. *Int. J. Dev. Biol.* **42,** 955–976.

Eggenschwiler, J., Ludwig, T., Fisher, P., Leighton, P. A., Tilghman, S. M., and Efstratiadis, A. (1997). Mouse mutant embryos overexpressing IGF-II exhibit phenotypic features of the Beckwith–Wiedemann and Simpson–Golabi–Behmel syndromes. *Genes Dev.* **11,** 3128–3142.

Farquharson, C., Lester, D., Seawright, E., Jefferies, D., and Houston, B. (1999). Microtubules are potential regulators of growth-

plate chondrocyte differentiation and hypertrophy. *Bone* **25,** 405–412.

Floyd, W. E., Zaleske, D. J., Schiller, A. L., Trahan, C., and Mankin, H. J. (1987). Vascular events associated with the appearance of the secondary center of ossification in the murine distal femoral epiphysis. *J. Bone Joint Surg. Am.* **69,** 185–190.

Fowden, A. L. (1995). Endocrine regulation of fetal growth. *Reprod. Fertil. Dev.* **7,** 351–363.

Frick, G. P., Tai, L. R., and Goodman, H. M. (1994). Subcellular distribution of the long and short isoforms of the growth hormone (GH) receptor in rat adipocytes: Both isoforms participate in specific binding of GH. *Endocrinology* **134,** 307–314.

Frischmeyer, P. A., and Dietz, H. C. (1999). Nonsense-mediated mRNA decay in health and disease. *Hum. Mol. Genet.* **8,** 1893–1900.

Garcia-Aragon, J., Lobie, P. E., Muscat, G. E., Gobius, K. S., Norstedt, G., and Waters, M. J. (1992). Prenatal expression of the growth hormone (GH) receptor/binding protein in the rat: A role for GH in embryonic and fetal development? *Development* **114,** 869–876.

Gibson, G. (1998). Active role of chondrocyte apoptosis in endochondral ossification. *Microsc. Res. Tech.* **43,** 191–204.

Goedbloed, J. F. (1974). The embryonic and postnatal growth of rat and mouse. II. The growth of the whole animal during the first 24 days after birth in two inbred mouse strains (CPB-S and DBA-2). *Acta Anat.* **87,** 209–247.

Goedbloed, J. F. (1975). The embryonic and postnatal growth of rat and mouse. III. Growth of the whole animal in the puberty, adult, and senescence phases in two inbred mouse strains (CPB-S and DBA/2). Exponential growth, sudden changes in the growth rate, and a model for the regulation of the mitotic rate. *Acta Anat.* **91,** 1–56.

Göthe, S., Wang, Z., Ng, L., Kindblom, J. M., Barros, A. C., Ohlsson, C., Vennstrom, B., and Forrest, D. (1999). Mice devoid of all known thyroid hormone receptors are viable but exhibit disorders of the pituitary–thyroid axis, growth, and bone maturation. *Genes Dev.* **13,** 1329–1341.

Green, H., Morikawa, M., and Nixon, T. (1985). A dual effector theory of growth-hormone action. *Differentiation* **29,** 195–198.

Hahn, T. M., Copeland, K. C., and Woo, S. L. (1996). Phenotypic correction of dwarfism by constitutive expression of growth hormone. *Endocrinology* **137,** 4988–4993.

Hanna, J. D., Santos, F., Foreman, J. W., Chan, J. C., and Han, V. K. (1995). Insulin-like growth factor-I gene expression in the tibial epiphyseal growth plate of growth hormone-treated uremic rats. *Kidney Int.* **47,** 1374–1382.

Herrington, J., Smit, L. S., Schwartz, J., and Carter-Su, C. (2000). The role of STAT proteins in growth hormone signaling. *Oncogene* **19,** 2585–2597.

Horton, W. E., Feng, L., and Adam, C. (1998). Chondrocyte apoptosis in development, aging and disease. *Matrix Biol.* **17,** 107–115.

Hunziker, E. B. (1994). Mechanism of longitudinal bone growth and its regulation by growth plate chondrocytes. *Microsc. Res Tech.* **28,** 505–519.

Hunziker, E. B., Wagner, J., and Zapf, J. (1994). Differential effects of insulin-like growth factor I and growth hormone on developmental stages of rat growth plate chondrocytes in vivo. *J. Clin. Invest.* **93,** 1078–1086.

Hynes, M. A., Van Wyk, J. J., Brooks, P. J., D'Ercole, A. J., Jansen, M., and Lund, P. K. (1987). Growth hormone dependence of somatomedin-C/insulin-like growth factor-I and insulin-like

growth factor-II messenger ribonucleic acids. *Mol. Endocrinol.* **1,** 233–242.

Isaksson, O. G., Jansson, J. O., and Gause, I. A. (1982). Growth hormone stimulates longitudinal bone growth directly. *Science* **216,** 1237–1239.

Isaksson, O. G., Lindahl, A., Nilsson, A., and Isgaard, J. (1987). Mechanism of the stimulatory effect of growth hormone on longitudinal bone growth. *Endocr. Rev.* **8,** 426–438.

Itier, J. M., Tremp, G. L., Leonard, J. F., Multon, M. C., Ret, G., Schweighoffer, F., Tocque, B., Bluet-Pajot, M. T., Cormier, V., and Dautry, F. (1998). Imprinted gene in postnatal growth role. *Nature* **393,** 125–126.

Iwasaki, M., Le, A. X., and Helms, J. A. (1997). Expression of Indian hedgehog, bone morphogenetic protein 6 and Gli during skeletal morphogenesis. *Mech. Dev.* **69,** 197–202.

Johnson, M. L. (1933). The time and order of appearance of ossification centers in the albino mouse. *Am. J. Anat.* **52,** 241–271.

Joseph, B. K., Marks, S. C., Hume, D. A., Waters, M. J., and Symons, A. L. (1999). Insulin-like growth factor-I (IGF-I) and IGF-I receptor (IGF-IR) immunoreactivity in normal and osteopetrotic (toothless, tl/tl) rat tibia. *Growth Factors* **16,** 279–291.

Jürgens, K. D., Bartels, H., and Bartels, R. (1981). Blood oxygen transport and organ weights of small bats and small non-flying mammals. *Respir. Physiol.* **45,** 243–260.

Kember, N. F. (1971). Cell population kinetics of bone growth: The first ten years of autoradiographic studies with tritiated thymidine. *Clin. Orthop.* **76,** 213–230.

Kember, N. F. (1978). Cell kinetics and the control of growth in long bones. *Cell Tissue Kinet.* **11,** 477–485.

Kember, N. F. (1993). Cell kinetics and the control of bone growth. *Acta Paediatr.* **82**(Suppl. 391), 61–65.

Kikkawa, M., Imai, S., and Hukuda, S. (2000). Altered postnatal expression of insulin-like growth factor-I (IGF-I) and type X collagen preceding the Perthes' disease-like lesion of a rat model. *J. Bone Miner. Res.* **15,** 111–119.

Kioussi, C., Carrière, C., and Rosenfeld, M. G. (1999). A model for the development of the hypothalamic–pituitary axis: Transcribing the hypophysis. *Mech. Dev.* **81,** 23–35.

Koops, W. J. (1986). Multiphasic growth curve analysis. *Growth* **50,** 169–177.

Koops, W. J., Grossman, M., and Michalska, E. (1987). Multiphasic growth curve analysis in mice. *Growth* **51,** 372–382.

Kopchick, J. J., and Laron, Z. (1999). Is the Laron mouse an accurate model of Laron syndrome? *Mol. Genet. Metab.* **68,** 232–236.

Laron, Z. (1999). Natural history of the classical form of primary growth hormone (GH) resistance (Laron syndrome). *J. Pediatr. Endocrinol. Metab.* **12**(Suppl. 1), 231–249.

Lazowski, D. A., Fraher, L. J., Hodsman, A., Steer, B., Modrowski, D., and Han, V. K. (1994). Regional variation of insulin-like growth factor-I gene expression in mature rat bone and cartilage. *Bone* **15,** 563–576.

Lee, K., Deeds, J. D., Chiba, S., Un-No, M., Bond, A. T., and Segre, G. V. (1994). Parathyroid hormone induces sequential c-fos expression in bone cells *in vivo: In situ* localization of its receptor and c-*fos* messenger ribonucleic acids. *Endocrinology* **134,** 441–450.

Lee, Y. H., Sauer, B., and Gonzalez, F. J. (1998). Laron dwarfism and non-insulin-dependent diabetes mellitus in the Hnf-1alpha knockout mouse. *Mol. Cell. Biol.* **18,** 3059–3068.

Lemmey, A. B., Glassford, J., Flick-Smith, H. C., Holly, J. M., and Pell, J. M. (1997). Differential regulation of tissue insulin-like

growth factor-binding protein (IGFBP)-3, IGF-I and IGF type1 receptor mRNA levels, and serum IGF-I and IGFBP concentrations by growth hormone and IGF-I. *J. Endocrinol.* **154,** 319–328.

Liu, J. P., Baker, J., Perkins, A. S., Robertson, E. J., and Efstratiadis, A. (1993). Mice carrying null mutations of the genes encoding insulin-like growth factor I (Igf-1) and type 1 IGF receptor (*Igf1*r). *Cell* **75,** 59–72.

Liu, J. L, and LeRoith, D. (1999). Insulin-like growth factor I is essential for postnatal growth in response to growth hormone. *Endocrinology* **140,** 5178–5184.

MacLeod, J. N., Pampori, N. A., and Shapiro, B. H. (1991). Sex differences in the ultradian pattern of plasma growth hormone concentrations in mice. *J. Endocrinol.* **131,** 395–399.

Maor, G., and Karnieli, E. (1999). The insulin-sensitive glucose transporter (GLUT4) is involved in early bone growth in control and diabetic mice, but is regulated through the insulin-like growth factor I receptor. *Endocrinology* **140,** 1841–1851.

Mathews, L. S., Norstedt, G., and Palmiter, R. D. (1986). Regulation of insulin-like growth factor I gene expression by growth hormone. *Proc. Natl. Acad. Sci. USA* **83,** 9343–9347.

Mathews, L. S., Hammer, R. E., Behringer, R. R., D'Ercole, A. J., Bell, G. I., Brinster, R. L., and Palmiter, R. D. (1988). Growth enhancement of transgenic mice expressing human insulin-like growth factor I. *Endocrinology* **123,** 2827–2833.

Metón, I., Boot, E. P., Sussenbach, J. S., and Steenbergh, P. H. (1999). Growth hormone induces insulin-like growth factor-I gene transcription by a synergistic action of STAT5 and HNF-1α. *FEBS Lett.* **444,** 155–159.

Moffat, J. G., Edens, A., and Talamantes, F. (1999). Structure and expression of the mouse growth hormone receptor/growth hormone binding protein gene. *J. Mol. Endocrinol.* **23,** 33–44.

Murphy, L. J., Bell, G. I., Duckworth, M. L., and Friesen, H. G. (1987). Identification, characterization, and regulation of a rat complementary deoxyribonucleic acid which encodes insulin-like growth factor-I. *Endocrinology* **121,** 684–691.

Nilsson, A., Isgaard, J., Lindahl, A., Dahlstrom, A., Skottner, A., and Isaksson, O. G. (1986). Regulation by growth hormone of number of chondrocytes containing IGF-I in rat growth plate. *Science* **233,** 571–574.

Nilsson, A., Carlsson, B., Isgaard, J., Isaksson, O. G., and Rymo, L. (1990). Regulation by GH of insulin-like growth factor-I mRNA expression in rat epiphyseal growth plate as studied with in-situ hybridization. *J. Endocrinol.* **125,** 67–74.

Nuttall, J. D., Brumfield, L. K., Fazzalari, N. L., Hopwood, J. J., and Byers, S. (1999). Histomorphometric analysis of the tibial growth plate in a feline model of mucopolysaccharidosis type VI. *Calcif. Tissue Int.* **65,** 47–52.

Ohlsson, C., Nilsson, A., Isaksson, O., and Lindahl, A. (1992). Growth hormone induces multiplication of the slowly cycling germinal cells of the rat tibial growth plate. *Proc. Natl. Acad. Sci. USA* **89,** 9826–9830.

Ohlsson, C., Bengtsson, B.-A., Isaksson, O. G. P., Andreassen, T. T., and Slootweg, M. C. (1998). Growth hormone and bone. *Endocr. Rev.* **19,** 55–79.

Pantaleon, M., Whiteside, E. J., Harvey, M. B., Barnard, R. T., Waters, M. J., and Kaye, P. L. (1997). Functional growth hormone (GH) receptors and GH are expressed by preimplantation mouse embryos: A role for GH in early embryogenesis? *Proc. Natl. Acad. Sci. USA* **94,** 5125–5130.

Patton, J. T., and Kaufman, M. H. (1995). The timing of ossification of the limb bones, and growth rates of various long bones of the fore and hind limbs of the prenatal and early postnatal laboratory mouse. *J. Anat.* **186,** 175–185.

Postic, C., and Magnuson, M. A. (2000). DNA excision in liver by an albumin-Cre transgene occurs progressively with age. *Genesis* **26,** 149–150.

Price, J. S., Oyajobi, B. O., and Russell, R. G. (1994). The cell biology of bone growth. *Eur. J. Clin. Nutr.* **48** (Suppl. 1), S131–S149.

Rihani-Bisharat, S., Maor, G., and Lewinson, D. (1998). *In vivo* anabolic effects of parathyroid hormone (PTH) 28-48 and N-terminal fragments of PTH and PTH-related protein on neonatal mouse bones. *Endocrinology* **139,** 974–981.

Roberts, C. T., Lasky, S. R., Lowe, W. L., Jr., Seaman, W. T., and LeRoith, D. (1987). Molecular cloning of rat insulin-like growth factor I complementary deoxyribonucleic acids: Differential messenger ribonucleic acid processing and regulation by growth hormone in extrahepatic tissues. *Mol. Endocrinol.* **1,** 243–248.

Rosenfeld, R. G., Rosenbloom, A. L., and Guevara-Aguirre, J. (1994). Growth hormone (GH) insensitivity due to primary GH receptor deficiency. *Endocr. Rev.* **15,** 369–390.

Salmon, W. D., and Burkhalter, V. J. (1997). Stimulation of sulfate and thymidine incorporation into hypophysectomized rat cartilage by growth hormone and insulin-like growth factor-I in vitro: The somatomedin hypothesis revisited. *J. Lab. Clin. Med.* **129,** 430–438.

Salmon, W. D., and Daughaday, W. H. (1957). A hormonally controlled serum factor which stimulates sulfate incorporation by cartilage in vitro. *J. Lab. Clin. Med.* **49,** 825–836.

Scanes, C. G., and Daughaday, W. H. (1995). Growth hormone action: Growth. *In* "Growth Hormone" (S. Harvey, C. G. Scanes, and W. H. Daughaday, Eds.), pp. 351–370. CRC Press, Boca Raton, FL.

Schaeren-Wiemers, N., and Gerfin-Moser, A. (1993). A single protocol to detect transcripts of various types and expression levels in neural tissue and cultured cells: In situ hybridization using digoxigenin-labelled cRNA probes. *Histochemistry* **100,** 431–440.

Schlechter, N. L., Russell, S. M., Greenberg, S., Spencer, E. M., and Nicoll, C. S. (1986). A direct growth effect of growth hormone in rat hindlimb shown by arterial infusion. *Am. J. Physiol.* **250,** E231–E235.

Shea, B. T., Hammer, R. E., and Brinster, R. L. (1987). Growth allometry of the organs in giant transgenic mice. *Endocrinology* **121,** 1924–1930.

Shinar, D. M., Endo, N., Halperin, D., Rodan, G. A., and Weinreb, M. (1993). Differential expression of insulin-like growth factor-I (IGF-I) and IGF-II messenger ribonucleic acid in growing rat bone. *Endocrinology* **132,** 1158–1167.

Silbermann, M., and Kedar, T. (1977). Observations on the growth of the normal male mouse. *Acta Anat.* **98,** 253–263.

Sjögren, K., Liu, J. L., Blad, K., Skrtic, S., Vidal, O., Wallenius, V., LeRoith, D., Tornell, J., Isaksson, O. G., Jansson, J. O., and Ohlsson, C. (1999). Liver-derived insulin-like growth factor I (IGF-I) is the principal source of IGF-I in blood but is not required for postnatal body growth in mice. *Proc. Natl. Acad. Sci. USA* **96,** 7088–7092.

Sjögren, K., Bohlooly, Y. M., Olsson, B., Coschigano, K., Tornell, J., Mohan, S., Isaksson, O. G., Baumann, G., Kopchick, J., and Ohlsson, C. (2000). Disproportional skeletal growth and markedly decreased bone mineral content in growth hormone receptor −/− mice. *Biochem. Biophys. Res. Commun.* **267,** 603–608.

Smith, W. C., and Talamantes, F. (1987). Identification and characterization of a heterogeneous population of growth hormone

receptors in mouse hepatic membranes. *J. Biol. Chem.* **262,** 2213–2219.

Spiteri-Grech, J., Bartlett, J. M., and Nieschlag, E. (1991). Regulation of testicular insulin-like growth factor-I in pubertal growth hormone-deficient male rats. *J. Endocrinol.* **131,** 279–285.

Sugisaki, T., Yamada, T., Takamatsu, K., and Noguchi, T. (1993). The influence of endocrine factors on the serum concentrations of insulin-like growth factor-I (IGF-I) and IGF-binding proteins. *J. Endocrinol.* **138,** 467–477.

Symons, A. L., Mackay, C. A., Leong, K., Hume, D. A., Waters, M. J., and Marks, S. C. (1996). Decreased growth hormone receptor expression in long bones from the toothless (osteopetrotic) rats and restoration by treatment with colony-stimulating factor-1. *Growth Factors* **13,** 1–10.

Tannembaum, G. S., Guyda, H. J., and Posner, B. I. (1983). Insulin-like growth factors: A role in growth hormone negative feedback and body weight regulation via brain. *Science* **220,** 77–79.

Teglund, S., McKay, C., Schuetz, E., van Deursen, J. M., Stravopodis, D., Wang, D., Brown, M., Bodner, S., Grosveld, G., and Ihle, J. N. (1998). Stat5a and Stat5b proteins have essential and nonessential, or redundant, roles in cytokine responses. *Cell* **93,** 841–850.

Udy, G. B., Towers, R. P., Snell, R. G., Wilkins, R. J., Park, S. H., Ram, P. A., Waxman, D. J., and Davey, H. W. (1997). Requirement of STAT5b for sexual dimorphism of body growth rates and liver gene expression. *Proc. Natl. Acad. Sci. USA* **94,** 7239–7244.

van Buul-Offers, S., Ueda, I., and Van den Brande, J. L. (1986). Biosynthetic somatomedin C (SM-C/IGF-I) increases the length and weight of Snell dwarf mice. *Pediatr. Res.* **20,** 825–827.

van Buul-Offers, S., Hoogerbrugge, C. M., Branger, J., Feijlbrief, M., and Van den Brande, J. L. (1988). Growth-stimulating effects of somatomedin-/insulin-like peptides in Snell dwarf mice. *Horm. Res.* **29,** 229–236.

van Buul-Offers, S., Van Kleffens, M., Koster, J. G., Lindenbergh-Kortleve, D. J., Gresnigt, M. G., Drop, S. L., Hoogerbrugge, C. M., Bloemen, R. J., Koedam, J. A., and Van Neck, J. W. (2000). Human insulin-like growth factor (IGF) binding protein-1 inhibits IGF-I-stimulated body growth but stimulates growth of the kidney in Snell dwarf mice. *Endocrinology* **141,** 1493–1499.

Vanky, P., Brockstedt, U., Hjerpe, A., and Wikstrom, B. (1998). Kinetic studies on epiphyseal growth cartilage in the normal mouse. *Bone* **22,** 331–339.

Vidal, N. O. A., Ekberg, S., Enerbäck, S., Lindahl, A., and Ohlsson, C. (1997). The CCAAT/enhancer-binding protein-α is expressed in the germinal layer of the growth plate: Colocalisation with the growth hormone receptor. *J. Endocrinol.* **155,** 433–441.

Vu, T. H., Shipley, J. M., Bergers, G., Berger, J. E., Helms, J. A., Hanahan, D., Shapiro, S. D., Senior, R. M., and Werb, Z. (1998). MMP-9/gelatinase B is a key regulator of growth plate angiogenesis and apoptosis of hypertrophic chondrocytes. *Cell* **93,** 411–422.

Walker, K. V. R., and Kember, N. F. (1972a). Cell kinetics of growth cartilage in the rat tibia. I. Measurements in young male rats. *Cell Tissue Kinet.* **5,** 401–408.

Walker, K. V. R., and Kember, N. F. (1972b). Cell kinetics of growth cartilage in the rat tibia. II. Measurements during ageing. *Cell Tissue Kinet.* **5,** 409–419.

Wang, E., Wang, J., Chin, E., Zhou, J., and Bondy, C. A. (1995). Cellular patterns of insulin-like growth factor system gene expression in murine chondrogenesis and osteogenesis. *Endocrinology* **136,** 2741–2751.

Wang, J., Zhou, J., and Bondy, C. A. (1999). *Igf1* promotes longitudinal bone growth by insulin-like actions augmenting chondrocyte hypertrophy. *FASEB J.* **13,** 1985–1990.

Watkins-Chow, D. E., and Camper, S. A. (1998). How many homeobox genes does it take to make a pituitary gland? *Trends Genet.* **14,** 284–290.

Werther, G. A., Haynes, K. M., Barnard, R., and Waters, M. J. (1990). Visual demonstration of growth hormone receptors on human growth plate chondrocytes. *J. Clin. Endocrinol. Metab.* **70,** 1725–1731.

Williams, G. R., Robson, H., and Shalet, S. M. (1998). Thyroid hormone actions on cartilage and bone: Interactions with other hormones at the epiphyseal plate and effects on linear growth. *J. Endocrinol.* **157,** 391–403.

Winick, M., and Grant, P. (1968). Cellular growth in the organs of the hypopituitary dwarf mouse. *Endocrinology* **83,** 544–547.

Wirtschafter, Z. T. (1960). "The Genesis of the Mouse Skeleton: A Laboratory Atlas." Thomas, Springfield, IL.

Won, W., and Powell-Braxton, L. (1998). Insulin-like growth factor gene targeting. *In* "Molecular Mechanisms to Regulate the Activities of Insulin-like Growth Factors" (K. Takano, N. Hizuka, and S. I. Takahashi, Eds.), pp. 57–63. Elsevier, Amsterdam.

Xu, J., Liao, L., Ning, G., Yoshida-Komiya, H., Deng, C., and O'Malley, B. W. (2000). The steroid receptor coactivator SRC-3 (p/CIP/RAC3/AIB1/ACTR/TRAM-1) is required for normal growth, puberty, female reproductive function, and mammary gland development. *Proc. Natl. Acad. Sci. USA* **97,** 6379–6384.

Yakar, S., Liu, J. L., Stannard, B., Butler, A., Accili, D., Sauer, B., and LeRoith, D. (1999). Normal growth and development in the absence of hepatic insulin-like growth factor I. *Proc. Natl. Acad. Sci. USA* **96,** 7324–7329.

Yamashita, S., and Melmed, S. (1986). Insulin-like growth factor I action on rat anterior pituitary cells: Suppression of growth hormone secretion and messenger ribonucleic acid levels. *Endocrinology* **118,** 176–182.

Zapf, J. (1998). Growth promotion by insulin-like growth factor I in hypophysectomized and diabetic rats. *Mol. Cell. Endocrinol.* **140,** 143–149.

Zhou, Y., Xu, B. C., Maheshwari, H. G., He, L., Reed, M., Lozykowski, M., Okada, S., Cataldo, L., Coschigano, K., Wagner, T. E., Baumann, G., and Kopchick, J. J. (1997). A mammalian model for Laron syndrome produced by targeted disruption of the mouse growth hormone receptor/binding protein gene (the Laron mouse). *Proc. Natl. Acad. Sci. USA* **94,** 13215–13220.